PROSTAGLANDIN J2: ITS ROLE IN PROTEIN AGGREGATION AND CYTOSKELETAL INTEGRITY

by

Kenyon D. Ogburn

A dissertation submitted to the Graduate Faculty in Biology in partial fulfillment of the requirements for the degree of Doctor of Philosophy, The City University of New York

UMI Number: 3213268

ProQuest Information and Learning Company
300 North Zeeb Road
P.O. Box 1346
Ann Arbor, MI 48106-1346

This Manuscript has been read and accepted by the Graduate Faculty in Biology in satisfaction of the dissertation requirement for the degree of Doctor of Philosophy

Date	**Dr. MARIA FIGUEIREDO-PEREIRA** (Hunter College, **Chair of Examining Committee**)
Date	**Dr. Richard Chappell** **Executive Officer**
	Dr. Derrick Brazill (Hunter College)
	Dr. Serge Przedborski (Columbia University Medical Center)
	Dr. Nikolaos Robakis (Mount Sinai School of Medicine)
	Dr. Patricia Rockwell (Hunter College)

Supervisory Committee

THE CITY UNIVERSITY OF NEW YORK

Abstract

PROSTAGLANDIN J2: ITS ROLE IN PROTEIN AGGREGATION AND CYTOSKELETAL INTEGRITY

by

Kenyon D. Ogburn

Advisor: Dr. Maria E. Figueiredo-Pereira

Two fundamental aspects of many neurodegenerative disorders, such as Alzheimer's disease (AD) and Parkinson's disease (PD) are the presence of (1) signs of inflammation and (2) neuronal inclusions containing ubiquitinated protein aggregates. The relationship between these two pathological characteristics and their contribution to neurodegeneration are poorly defined.

This research was undertaken to investigate the impact of a product of inflammation, i.e. prostaglandin J2 (PGJ2), on neuronal homeostasis and on the development of ubiquitinated protein aggregates. We chose to investigate the effects of PGJ2 because it is an endogenous ligand that is a metabolite of PGD2, the most prominent prostaglandin in the mammalian brain.

Our data show that the "inflammatory mediator" PGJ2 (1) compromises an enzymatic activity associated with detoxification pathways thus exacerbating neuronal damage and (2) mediates protein aggregation in neuronal cells by perturbing (a) cytoskeletal integrity and (b) proteasome activity.

In conclusion, these data strongly support the notion that neurotoxic products of inflammation, such as PGJ2, recapitulate many of the pathological processes relevant to neurodegenerative disorders such as AD and PD. Inflammation is thus likely to play a pivotal role in numerous neurodegenerative disorders. Traditional anti-inflammatory drugs that target cyclooxygenase activities have limited therapeutic use in neurodegeneration because of their severe side effects after long-term use. The development of novel anti-inflammatory drugs more specifically aimed at targets downstream from cyclooxygenases may prove to be more effective neuroprotective agents in multiple forms of neurodegenerative diseases.

Acknowledgements

Table of Contents

Table of Figures

List of Abbreviations

3MT 3-methoxytyramine

15d-PGJ2 15-deoxy-Δ12,14-prostaglandin J2

AAA ATPases associated with diverse cellular activities

AD Alzheimer's disease

AID Acidic interaction domain

ALS Amyotrophic lateral sclerosis

CNS Central nervous system

COMT Catechol-*O*-methyltransferase

COX-1 Cyclooxygenase-1

COX-2 Cyclooxygenase-2

CP Core particle

DA Dopamine

DAPI 4’,6-Diamidino-2-phenylindole

DMSO Dimethylsulfoxide

DOPAC 3,4-di-hydroxy-phenyl-acetic acid

DTNB 5,5'-Dithio-bis(2-nitrobenzoic acid)

DTT Dithiothreitol

ERK Extracellular regulated kinase

ER Endoplasmic reticulum

GAB General actin buffer

GFP Green fluorescent protein

GTB General tubulin buffer

HNE 4-Hydroxy-2-nonenal

HPLC High performance liquid chromatography

HVA Homovanillic acid

iNOS Inducible nitric oxide synthase

JNK Jun N-terminal kinase

LBs Lewy bodies

MAO Monoamine oxidase

MAPK Mitogen-activated protein kinase

MB-COMT Membrane-bound COMT

MEM Minimal essential media

MPP^+ 1-methyl-4-phenylpyridinium ion

MTOC Microtubule organizing center

MTT 3-(4,5-Dimethylthiazol2-yl)-2,5-diphenyl-tetrazolium

p62 Sequestosome

PBS Phosphate-buffered saline

PCA Perchloric acid

PD Parkinson's disease

PGs Prostaglandins

PGD2 Prostaglandin D2

PGG2 Prostaglandin G2

PGH2 Prostaglandin H2

PGJ2 J2 prostaglandins

PPARγ Proliferator-activated receptor

PSI N-benzyloxycarbonyl-Ile-Glu(O-t-butyl)-Ala-leucinal

RIP Receptor interactive protein

RNAi RNA interference

ROS Reactive oxygen species

RP Regulatory particle

RT-PCR Reverse-transcription-polymerase chain reaction

SAM *S*-adenosyl-L-methionine

S-COMT Soluble-COMT

SNpc Substantia nigra pars compacta

TRAF6 Tumor necrosis factor receptor-associated factor 6

TX Triton X-100

UBL Ubiquitin-like domains

UCH Ubiquitin-carboxy terminal

UPP Ubiquitin-proteasome pathway

Z-LL-CHO Calpain/cathepsin inhibitor (N-benzyloxycarbonyl-Leu-leucinal)

CHAPTER I

INTRODUCTION

Protein deposits containing ubiquitinated proteins are detected in non-pathologic aging [1] as well as in a variety of age-related neurodegenerative disorders including Alzheimer's disease (AD), Parkinson's disease (PD) and amyotrophic lateral sclerosis (ALS), to name a few [2]. All of these protein deposits contain ubiquitinated proteins but their major structural components vary from cell type to cell type. For example, microtubule associated *tau* proteins are found in cortical neurofibrillary tangles and α-synuclein in dopaminergic Lewy bodies [3]. The presence of aggregated ubiquitinated proteins in inclusion bodies indicates impairment of the ubiquitin-proteasome pathway (UPP) or structural changes in protein substrates impeding their degradation. The mechanisms causing the aggregation of ubiquitinated proteins have to be addressed in order to understand the overall molecular disease processes of these neurological conditions.

Inflammation and oxidative stress may be critical contributors to the intracellular aggregation of ubiquitinated proteins that evade degradation by the UPP [5]. Chronic inflammation of the CNS has been implicated in a variety of neurodegenerative disorders. Notably, the spatial and temporal distribution of pro-inflammatory cyclooxygenase-2 (COX-2) correlates with neuropathological

changes in a wide variety of disorders including AD, PD and ALS [4]. These disorders, which exhibit signs of inflammation, are also associated with accumulation of ubiquitinated proteins in neuronal inclusions [5]. Notably, inflammatory processes occurring in the CNS differ from systemic inflammation. The order of events occurring in the CNS following a noxious insult includes: ***(i)*** immune cell proliferation, ***(ii)*** microglia activation, ***(iii)*** cytokine release and ***(iv)*** induction of tissue repair enzymes. Together, these responses are initiated as a defense mechanism to help limit cellular damage and repair the CNS [6]. Ironically, these same pro-inflammatory events can incite tissue damage in both acute and chronic CNS disorders.

The involvement of oxidative stress in neurodegeneration has gained support from increasing evidence of its role in neuronal death in disorders such as AD and PD. Studies with autopsied brains of AD patients show a co-localization of high levels of oxidative stress products with neurofibrillary tangles and senile plaques [7]. Signs of oxidative stress, such as lipid peroxidation, increased protein carbonyls and a decline in reduced glutathione, were also detected in the ***substantia nigra*** in brains of PD patients [8]. Oxidative stress, especially the

production of free radicals, promotes partial unfolding of cellular proteins resulting in the exposure of previously buried hydrophobic domains to ubiquitin-conjugating [9], as well as to proteolytic enzymes [10;11]. One important cellular response to oxidative stress is an increase in intracellular proteolysis by the proteasome.

To provide a general overview of the current information available on the relationship among neuroinflammation, oxidative stress and the aggregation of ubiquitinated proteins in neurodegeneration, the following topics will be addressed: ***(i)*** Inducers of oxidative stress; ***(ii)*** Degradation of oxidatively modified proteins; ***(iii)*** Inflammation and protein aggregation. The overall aim of this introduction is to provide strong support for the view that CNS inflammation and oxidative stress are critical contributors to the formation of inclusion bodies detected in most neurodegenerative disorders.

1.1. INDUCERS OF OXIDATIVE STRESS

1.1.1. Aerobic Respiration

Reactive oxygen species (ROS), such as superoxide and hydrogen peroxide, are produced by mitochondria during respiration, rendering all aerobic organisms susceptible to

oxidative stress. Of the total oxygen consumed during respiration, approximately 2% ends up as ROS, but this amount may vary depending on exposure to various stress conditions, such as environmental pollutants (metals and xenobiotics) and inflammatory cytokines. The brain is considered to be abnormally sensitive to oxidative damage because ***(i)*** it is enriched in the more easily peroxidizable fatty acids, ***(ii)*** relative to its small weight, it consumes an excessive fraction of the body's total oxygen consumption and ***(iii)*** it is not particularly enriched in antioxidant defenses [15]. For example, the brain is low in catalase activity, containing about 10% of liver catalase. In addition, certain regions of the human brain are enriched in iron/ascorbate. If tissue organizational disruption occurs, the iron/ascorbate mixture becomes an abnormally potent pro-oxidant for brain membranes [15].

Agents that impair mitochondrial activity decrease ATP production and promote ROS formation. These cytotoxic agents change the redox equilibrium and may, for example, increase the levels of mitochondrial quinones such as Coenzyme Q_{12}. Coenzyme Q_{12} is essential for maintaining the proton gradient across the mitochondrial membrane. However, high levels of quinones elevate ROS production. Indeed, higher concentrations of quinones are found in the brains

of AD patients compared to normal controls, supporting a role for these compounds in the etiology of neurodegenerative diseases [16;17].

1.1.2. Inflammation

In the context of neurodegenerative disorders, neuroinflammation refers to any set of responses culminating in a COX-2-induced, pro-inflammatory response in CNS tissues. Cyclooxygenases (COX-1 or COX-2) are the rate-limiting enzymes in the synthesis of prostaglandins. In the first step, cyclooxygenases convert arachidonic acid to prostaglandin G2 (PGG2). Their peroxidase activity then converts PGG2 to prostaglandin H2 (PGH2), the parental prostanoid. PGH2 is subsequently converted to a variety of products including PGD2, PGE2, PGF2α, PGI2, and TxA2 by cell-specific isomerases and synthases. Under physiological conditions, the concentrations of prostaglandins in body fluids are in the pico-nanomolar range [18]. However, under inflammatory conditions, their concentrations may reach the micromolar range at the site of damage [19;20] and as such, they may act as pro-inflammatory mediators of oxidative stress.

Prostaglandins are primarily synthesized from arachidonic acid, which comes from membrane phospholipids and dietary sources [21;22]. In general, the majority of prostaglandins are considered pro-inflammatory; however, they may also be anti-inflammatory [19]. In a rat model of inflammation, COX-2 was initially pro-inflammatory by way of PGE2 synthesis. Conversely, during the resolution phase of inflammation, COX-2 was shown to be anti-inflammatory by way of PGD2 and 15d-PGJ2 production. Hence, the dual role of COX-2 is quite complex. PGD2 is the major prostanoid synthesized in the mammalian CNS. This prostanoid is unstable and readily undergoes both ***in vivo*** and ***in vitro*** non-enzymatic dehydration to generate biologically active cyclopentenone J2 prostaglandins, such as PGJ2, 12d-PGJ2 and 15d-PGJ2.

Some of the effects of J2 prostaglandins appear to be mediated by their interaction with an intranuclear target, the peroxisome proliferator-activated receptor (PPARγ). Several studies suggest that 15d-PGJ2 is a ligand for the PPARγ receptor [23]. PPARγ is a transcription factor found in many cell types, including neurons/microglia [24], macrophages/monocytes, myocytes, fibroblast, breast cells, and human bone marrow [25;26]. During a noxious insult, the stereotypic result of macrophage/microglia activation is

the production of various pro-inflammatory mediators. However, in the presence of 15d-PGJ2, the production of pro-inflammatory mediators such as IL-6, TNF-α, IL-1β and inducible nitric oxide synthase (iNOS) seems to be inhibited, thus favoring an anti-inflammatory response. In further support of this view, 15d-PGJ2 was found to inhibit IL-10 and IL-12 production by macrophages [27]. Other studies reported that PPARγ ligands induce monocytes/macrophages to respond in a pro-inflammatory manner by stimulating the expression of pro-inflammatory receptors, such as CD14 and CD11b/CD18 [28-31]. Clearly, the effects of PPARγ ligands, including 15d-PGJ2, are variable and may depend on factors such as intracellular concentrations, cell types and timing of activation of downstream targets that participate in the inflammatory response. In addition, J2 prostaglandins act through PPARγ-independent mechanisms, including activation of Erk (MAPK and JNK) pathways [32;33] and inhibition of the NFκB pathway [34;35]. This may account for the different effects of J2 prostaglandins and other PPARγ ligands [36].

J2 prostaglandins are unique among the prostaglandin family in that they have α,β-unsaturated carbonyl groups promoting Michael addition reactions with free sulfhydryl

groups of cysteines in glutathione and cellular proteins [37]. These cyclopentenone prostaglandins were shown to covalently modify several proteins, including the p50 subunit of NFκB, which may explain their anti-inflammatory effects [38]. They also modify thioredoxin reductase, an enzyme that protects against oxidative damage [39], and activate Ras, a small GTPase oncogene known to activate Erk signaling pathways [40].

Recent studies suggest that J2 prostaglandins play a role in the etiology of neurodegeneration. Specifically, the levels of 15d-PGJ2 were found to be elevated in spinal cord motor neurons of ALS patients [41]. Additionally, J2 prostaglandins were shown to be neurotoxic and pro-oxidant agents [42], up-regulate the expression of COX-2 [33], inhibit the activities of ubiquitin isopeptidase [43] and Ubiquitin-carboxyl terminal hydrolases (UCH)-L1 and UCH-L3 [44], induce the accumulation [42] and aggregation [44] of ubiquitinated proteins and induce neuronal apoptosis [45]. That UCH-L1 inhibition might be relevant to neurodegeneration is supported by the identification of a missense mutation in the gene encoding UCH-L1 in two siblings of a German family with autosomal-dominant familial PD [46]. As the UPP is a complex and tightly-

regulated system, there are undoubtedly other mechanisms by which J2 prostaglandins negatively affect the UPP.

1.1.3. Dopamine

Parkinson's disease (PD) is characterized by the selective degeneration of dopaminergic neurons of the nigrostriatal pathway. In PD, dopaminergic neuronal loss is accompanied by Lewy bodies (LBs), which are neuronal proteinaceous cytoplasmic inclusions [47;48]. The neuronal loss is also associated with the accumulation of highly-oxidized protein aggregates, often surrounded by microglia. Upon activation, microglia release a large amount of oxidizing species, thus initiating a potentially disastrous, inflammatory cytotoxic cycle. A compensatory mechanism initiated by the cell is to increase protein degradation [49].

Among the catecholamines, dopamine is the most susceptible to autooxidation that leads to ROS formation. This is because of its high rate of oxidation to an electron-deficient quinone and a slower rate of internal cyclization of the *o*-quinone structure [50]. Conditions that promote the intracellular accumulation of dopamine might thus lead to increased dopaminergic neuronal loss [51]. Susceptibility of dopaminergic neurons to oxidative

stress was shown in studies with rotenone, an environmental toxin linked specifically to PD [52].

Cyclooxygenases are also able to oxidize dopamine to dopamine quinone via their peroxidase activity. These enzymes will readily utilize dopamine as an electron donor to support their peroxidase activity generating an electron-deficient dopamine quinone as a byproduct. Dopamine quinone can then covalently bind to the sulfhydryl groups of cysteine residues on proteins. If the covalently modified cysteine is located at or near the protein active site, the binding of dopamine quinone will cause inactivation of protein function. If these protein functions are essential for cell viability, their inactivation may account for quinone-induced cytotoxicity [53].

PD pathogenesis is thus closely linked to oxidative stress [54]. Under such cytotoxic conditions, direct or indirect proteasome impairment might occur. This impairment could lead to the accumulation of cytotoxic proteins, disruption of neuronal function and ultimately cell death.

1.1.4. Proteotoxicity of Oxidative Stress

Understanding the sources of oxidative stress and how these conditions affect UPP activity and its substrates is

relevant to neurodegeneration. Strong oxidants like the various ROS resulting from oxidative stress damage the structure of cellular proteins [55] which, if not repaired, must be removed by proteolysis to prevent their accumulation and aggregation. One of the major roles of the proteasome is to remove oxidatively modified proteins. However, we still lack a clear understanding of how oxidatively modified proteins are targeted for proteasomal degradation. Some investigators support the notion that oxidatively modified proteins in cells are removed by the 20S proteasome independently of ubiquitination [56]. Nonetheless, it is not clear how these proteins would be recognized by the 20S proteasome. Others demonstrated that there is an accumulation of ubiquitin-protein conjugates as well as increases in ubiquitin-activating and ubiquitin-conjugating enzyme activities following episodes of oxidative stress. This suggests that the ubiquitination machinery is recruited to target oxidatively modified proteins for proteasomal degradation [57]. Understanding how oxidatively modified proteins are degraded is an important issue. Not only because the brain is considered to be unusually sensitive to oxidative damage, but also because many age-related neurodegenerative disorders

exhibit abnormal accumulation of oxidatively damaged proteins.

1.2. DEGRADATION OF OXIDATIVELY MODIFIED PROTEINS

It is likely that some or the majority of protein components of the cytoplasmic inclusion bodies detected in neurodegenerative disorders are aggregates of oxidatively modified proteins [58]. Although somewhat phenotypically-characterized, the biochemical mechanism leading to the formation of these protein aggregates remains poorly defined. It is well established that the ability of cells to degrade abnormal, mutated, or oxidized proteins is exceeded when the UPP is inhibited [59]. Thus, UPP impairment is likely to play an essential role in protein aggregation. These protein aggregates could themselves impair the UPP, generating a disastrous positive feedback loop. Initially, protein aggregates may not affect the UPP as the proteasome does attempt to rescue the cell from oxidative insults by degrading oxidatively modified proteins. The increased surface hydrophobicity of oxidatively modified proteins is postulated to make them more susceptible to proteasome mediated degradation [60-67]. This degradation is thought to result from recognition

of the hydrophobic moieties spanning the core of the protein to its surface. Exposure of these hydrophobic patches to the intracellular milieu is dependent on protein unfolding induced by its oxidation.

1.2.1. 20S *versus* 26S Proteasomes

Currently, it is uncertain whether it is the 26S or 20S proteasome that carries-out the *in vivo* degradation of oxidatively modified proteins. Several researchers support the notion that the 20S proteasome is sufficient for degradation of oxidatively modified proteins. It seems that degradation of the latter is ATP-independent [67] and that there is a decline in 26S proteasome activity following oxidative stress [68;69]. Furthermore, degradation of oxidatively modified proteins was not impaired in cell lines harboring an E1-Ub-activating enzyme deficient mutant [70]. Several concerns tamper this hypothesis. In the first place, these experiments involve *in vitro* assays that assess the accumulation of ubiquitinated proteins in cell-free lysates and under conditions that may not occur in an *in vivo* setting. This paradigm does not take into account possible factors that may be absent upon cell lysate preparation. Such factors might be required for the *in vivo* ubiquitin-mediated degradation of oxidatively modified

proteins. Secondly, lysozyme and ferritin were the only two substrates tested in these studies and they were exposed to high concentrations of H_2O_2, as the source of oxidative stress. These high H_2O_2 concentrations are unlikely to be ever attained intracellularly. Oxidative stress induced by H_2O_2 also affects the ubiquitin/proteasome pathway, either by directly decreasing the activity of the 20S or 26S proteasome [71-73], or by increasing the expression and activity of at least two members of the ubiquitination machinery, namely E1 and E2 enzymes [74]. The role of ubiquitination and ultimately, the involvement of the 26S proteasome in the degradation of oxidatively modified proteins should not be discounted.

1.2.2. Substrate Recognition by the 19S Regulatory Particle of the 26S Proteasome

The 26S proteasome consists of a 20S core particle (CP) and one or two 19S regulatory particles (RP) that cap the entry into the catalytic core [75]. The 19S RP facilitates recruitment of polyubiquitinated proteins to the 26S proteasome and their translocation into the 20S CP. The 19S RP is composed of two sub-complexes: the lid that is distal to the 20S CP and contains polyubiquitin binding

as well as deubiquitinating activities, and the base that is in contact with the pore of the 20S CP and consists of six ATPase and two non-ATPase subunits. The two latter subunits [Rpn1(S2) and Rpn2(S1)] interact with proteins that contain ubiquitin-like domains (UBL) and may participate in proteasomal substrate targeting [75]. In addition, at least two subunits of the 19S RP bind polyubiquitin chains directly, i.e. Rpn10 (S5a) and Rpt5 (S6'), but their role in substrate targeting remains undefined [75]. It is clear that recognition of substrates by the proteasome is facilitated by its 19S RP. This form of proteasome-substrate recognition might be compromised under stress conditions, such as oxidative stress, thus impairing the degradation of proteasomal substrates and leading to their aggregation in neuronal cells [76].

1.2.3. Modifications of the 19S Regulatory Particle of the 26S Proteasome

To address the mechanism underlying cell death induced by oxidative stress, human neuroblastoma SH-SY5Y cells were treated with an endogenous electrophile, i.e. 15d-PGJ2 that is a neurotoxic product of inflammation and a potent inducer of oxidative stress [76]. Through proteomic

analysis of oxidation-sensitive proteins, the 19S RP Rpt3(S6) subunit that has ATPase activity was shown to be one of the major targets of the 15d-PGJ2 induced protein carbonylation. Furthermore, Cu^{2+}/H_2O_2-treatment of SH-Y5Y cells also resulted in the oxidative modification of Rpt3(S6) [76]. As a mechanism to explain the metal-catalyzed oxidation of Rpt3(S6), it was postulated that Cu^{2+} binds to a specific metal-binding site on Rpt3(S6) and that Cu^{2+} may react with H_2O_2 to generate ROS. These ROS would then have the potential to oxidize neighboring amino acid residues, thereby generating carbonyl groups on the 19S RP subunit. These findings suggest that the Rpt3(S6) subunit may be one of various oxidation-sensitive subunits of the proteasome.

The Rpt3(S6) subunit of the 19S regulatory particle is one of six non-redundant ATPases all belonging to the AAA (ATPases associated with diverse cellular activities) superfamily [77]. Previous studies demonstrated that Rpt3(S6) may interact with additional 19S regulatory subunits, such as the Rpt5(S6') and Rpt1(S7) ATPases [78-81], and that these hexameric ATPase complexes are associated with substrate unfolding and translocation into the 20S CP. It is clear that 19S RP subunits are targets of oxidative insults in cells under conditions of oxidative

stress mediated by ROS or products of inflammation. Oxidation of 19S RP subunits could compromise the ability of the 26S proteasome to recognize and degrade polyubiquitinated proteins leading to the accumulation of cytotoxic, oxidatively-modified proteins.

In conclusion, oxidatively modified proteins may become polyubiquitinated and targeted for degradation by the 26S proteasome. However, their degradation might be perturbed if subunits of the 19S RP become oxidatively modified and lose their ability to bind and unfold substrates before they enter the 20S CP. This hypothesis is supported by the finding that Rpt3(S6) down-regulation by RNAi resulted in enhanced accumulation of ubiquitinated proteins [76]. Depending on the severity of the oxidative insult, the ability of the 26S proteasome to degrade oxidatively modified proteins might be only partially compromised. However, if the oxidative insult is chronic, the overall ability of the 26S proteasome to degrade oxidatively modified proteins may become totally compromised leading to accumulation of ubiquitinated proteins to toxic levels.

1.3. INFLAMMATION AND PROTEIN AGGREGATION

1.3.1. Oxidative Modifications

The levels of products of inflammation, such as J2 prostaglandins, may be increased rapidly in response to tissue injury or some other noxious insults. These high levels of J2 prostaglandins could exert their effect by generating ROS and thus promoting oxidative stress. Cellular proteins are susceptible to the oxidative modification of their amino acid side chains. This oxidation may radically alter the native conformation of proteins and, if not repaired, is likely to trigger their loss of function. Methionine and cysteine residues may be particularly susceptible to damage by ROS. While methionine is readily oxidized to methionine sulfoxide [82;83] cysteine sulfhydryl group oxidation may result in the formation of intra- or intermolecular disulfide bridges [84]. In addition, the prominent α,β-unsaturated ketones of J2 prostaglandins may undergo nucleophilic addition reactions with cysteine thiol groups. All of these chemical modifications can promote the aggregation of proteins or peptides, which is a hallmark of many neurodegenerative disorders. Increases in ROS, in conjunction with a decline in proteasome activity, both of which may be associated with oxidative stress and/or inflammation, may thus lead to

the progressive accumulation of oxidatively damaged and/or ubiquitinated proteins. Collectively, these could eventually lead to cellular dysfunction and neurodegeneration [84].

1.3.2. Inactivation and Sequestration of Metabolic Enzymes

Catechol-*O*-methyltransferase (COMT) is an enzyme responsible for inactivating catecholamine neurotransmitters, such as dopamine, as well as catechol hormones and catechol drugs like L-DOPA, α-methyl DOPA and isoprenaline [85;86]. Treatment of human neuroblastoma SK-N-SH cells with PGJ2, a product of inflammation, reduced the expression and activity of COMT and potentiated dopamine toxicity [87]. PGJ2 also triggered the formation of large perinuclear aggregates containing COMT, thus affecting its subcellular distribution. The latter was duplicated in rat primary cortical neurons. These results suggest that COMT-impairment induced by PGJ2-treatment, may increase the concentration of dopamine (or its metabolites) to neurotoxic levels and may thus be a potential risk factor in neurodegeneration. Furthermore, aggregation of metabolic enzymes, such as COMT as well as other proteins that may be essential for cell viability, has the potential

to seriously jeopardize cellular homeostasis. Under stress conditions, such as those induced by inflammation, sequestration of these proteins into aggregates may impair their activities and prevent them from promoting cell survival.

1.4. CONCLUSIONS

Inflammatory processes, in particular those attributed to chronic neuroinflammation are with no doubt implicated in neurodegenerative disorders such as AD and PD. However, there is an obvious gap in the knowledge of how endogenous products of inflammation alter underlying cellular mechanisms fundamental to neurodegeneration. Our overall hypothesis is that pro-inflammatory conditions may affect important cellular pathways involved in neuronal homeostasis through the production of J2 prostaglandins (PGJ2), which are derived from PGD2, the major prostaglandin synthesized in the mammalian CNS. Our studies presented herein address this premise by investigating the effects of PGJ2 on processes relevant to neurodegeneration.

CHAPTER II

PROSTAGLANDIN J2 REDUCES CATECHOL-*O*-METHYLTRANSFERASE ACTIVITY AND ENHANCES DOPAMINE TOXICITY IN NEURONAL CELLS

Kenyon D. Ogburn[1], Teodoro Bottiglieri[2], Zhiyou Wang[1] and Maria E. Figueiredo-Pereira[1*]

[1]Department of Biological Sciences, Hunter College of City University of New York, New York, New York 10021 and

[2]Baylor Institute of Metabolic Disease, Dallas, Texas 75226

2.1. ABSTRACT

There is clear evidence that an inflammatory reaction is mounted within the CNS following trauma, stroke, infection and seizures, thus augmenting brain damage. Furthermore, chronic inflammation of the CNS is implicated in many neurodegenerative disorders. However, the effects of products of inflammation on neuronal cells are poorly understood. Herein, we characterize the effects of a neurotoxic product of inflammation, prostaglandin J2 (PGJ2), on catechol-*O*-methyltransferase (COMT) in human dopaminergic-like neuroblastoma SK-N-SH cells and rat (P2) cortical neurons. COMT metabolizes catechols and catecholamines, a pathway relevant to neurodegeneration. PGJ2-treatment reduced the expression and activity of COMT, induced its sequestration into perinuclear aggregates and potentiated dopamine toxicity. The large COMT-aggregates were co-localized with the centrosome, suggesting an aggresome-like structure. Our results indicate that COMT-impairment induced by PGJ2-treatment may increase the concentration of dopamine (or its metabolites) to neurotoxic levels. Thus, COMT impairment following pro-inflammatory events may be a potential risk factor in neurodegeneration.

2.2. INTRODUCTION

Chronic inflammation of the CNS has been implicated in a variety of neurodegenerative disorders (reviewed in [88]). Notably, the spatial and temporal distribution of the pro-inflammatory cyclooxygenase-2 (COX-2) correlates with neuropathological changes in a wide variety of disorders including Parkinson's disease, Alzheimer's disease and amyotrophic lateral sclerosis (ALS) (reviewed in [4]). The brain expresses COX-1 and COX-2 under normal physiological conditions. However, the expression and activity of COX-2 are largely responsive to adverse stimuli, such as inflammation and physiologic imbalances [89]. COX-2 up-regulation following CNS injury is not restricted to neurons since COX-2 induction is also apparent in glia [90]. Although many studies support the notion that COX-2 is involved in neurodegeneration its contribution to the neurodegenerative process remains poorly defined.

Prostaglandins (PGs) are a family of structurally related molecules produced by cyclooxygenases in response to numerous extrinsic and intrinsic stimuli. Prostaglandins of the J2 series are derived from PGD2, the major prostanoid made in the mammalian CNS. PGD2 readily undergoes ***in vivo*** and ***in vitro*** non-enzymatic dehydration to

generate the biologically active cyclopentenone prostaglandins of the J2 series, which include PGJ2, Δ12-PGJ2 and 15-deoxy-Δ12,14-PGJ2 (15d-PGJ2) [91]. PGJ2 and its metabolites are not stored in tissues or cells. Their production increases with diverse stimuli. Although physiological concentrations of PGs in body fluids are in the pico-nanomolar range [92], their levels rise considerably under pathological conditions such as hyperthermia, infection and inflammation, reaching the micromolar range at the site of damage [93;94].

Our studies focus on PGs of the J2 series because initial studies established that these PGs are the most neurotoxic of the prostanoids that we tested, which also included PGA1, D2 and E2 [44]. In addition, recent reports suggest that prostaglandins of the J2 series play an important role in neurodegeneration. Accordingly, the levels of 15d-PGJ2, a PGJ2 metabolite, were found to be elevated in spinal cord motor neurons of ALS patients [45]. Moreover, prostaglandins of the J2 series trigger oxidative stress [42] and neuronal apoptosis [45].

Herein, we investigated the effects of PGJ2-treatment on catechol-*O*-methyltransferase (COMT). The main function of COMT is to inactivate catechol hormones, catecholamine neurotransmitters including dopamine, and many catechol

drugs such as L-DOPA, α-methyl DOPA and isoprenaline (reviewed in [85];[95]). Altered COMT activity was found to be associated with neurodegeneration. Accordingly, previous studies established that COMT activity is decreased in the spinal cord of patients with Huntington's disease [96]. Because of the involvement of COMT in the degradation of catechols and catecholamines, such as dopamine, it is easy to recognize that subtleties in COMT enzymatic activity might affect dopamine signaling (reviewed in [97]) and neurotoxicity, the latter due to its induction of oxidative stress (reviewed in [53]).

The *comt* gene encodes both the soluble (S-COMT) and membrane-bound (MB-COMT) forms of this enzyme. The human *comt* gene is found at chromosome 22 band q11.2 and consists of six exons, two of which (exons 1 and 2) are non-coding. Two distinct promoters regulate expression of the human comt gene: the distal promoter P2 encodes for MB-COMT and the proximal promoter P1 encodes for S-COMT (reviewed in [97]). S-COMT contains 221 amino acids and MB-COMT has a 50-residue amino-terminal extension that contains a hydrophobic membrane anchor region (reviewed in [98]). MB-COMT appears to be localized predominantly in neurons while S-COMT is in glia [99].

In the studies described herein, we demonstrate that treatment of neuronal cells with PGJ2 decreases COMT expression and activity, induces its sequestration into large perinuclear aggregates co-localized with the centrosome, and potentiates dopamine toxicity. Thus, we show that a product of inflammation, PGJ2, inactivates the detoxifying enzyme COMT. This inactivation may aggravate the effect of neurotoxic compounds, such as dopamine, a neurotransmitter that is chemically reactive and its oxidation products known to be highly toxic to neuronal cells. Our data support the notion that COMT impairment may be a potential risk factor in neurodegeneration.

2.3. MATERIALS AND METHODS

2.3.1. Materials - PGJ2 was from Cayman Chemical (Ann Arbor, MI), and 3-(4,5-Dimethylthiazol-2-yl)-2,5-diphenyl-tetrazolium bromide (MTT) and dopamine hydrochloride were from Sigma (St. Louis, MO). The following primary antibodies were used: rabbit polyclonal anti-COMT [1:10,000 (immunoblotting) and 1:500 (immunofluorescence) from Chemicon Int., Temecula, CA], mouse monoclonal anti-sequestosome (1:500, from BD Transduction Lab, San Diego, CA) and goat polyclonal anti-COX-1 [1:1,000

(immunoblotting) from Santa Cruz Biotechnology, Inc., Santa Cruz, CA]. The respective secondary antibodies with fluorophores (1:50) were from Jackson ImmunoResearch Laboratories, Inc. (West Grove, PA).

2.3.2. Cell cultures - SK-N-SH cells are a human dopaminergic-like neuroblastoma cell line derived from peripheral tissue [101]. They exhibit dopamine-β-hydroxylase activity as well as formaldehyde induced fluorescence indicative of intracellular catecholamines. The cells were maintained as described in [33]. Rat (P2) cortical neurons were prepared and maintained as described in [102].

2.3.3. Cell Treatments - Cell cultures were treated for 24h with DMSO (vehicle) or with increasing concentrations of PGJ2 in DMSO added directly to serum-containing medium. The final DMSO concentration in the medium was 0.5%. When specified, PGJ2 was added six hours prior to dopamine treatment, and the cultures were then incubated for an additional 24h in the presence of both agents. At the end of the incubation, all cultures were washed twice with phosphate buffered saline (PBS) and processed for the different assays as described below. Cell washes removed unattached cells, therefore, subsequent

assays were performed on adherent cells only.

2.3.4. Reverse Transcription-PCR Analysis - Total RNA was isolated with the RNAeasy Kit from Qiagen, Inc. (Valencia, CA). To perform each reverse-transcription-PCR, 1 μg of RNA/sample was reverse transcribed in a 25μl reaction (RETROscript reverse transcription kit from Ambion, Austin, TX), and 2μl of the resultant cDNA was amplified with gene-specific primers using the SuperTaq polymerase kit from Ambion (Austin, TX). The human-specific PCR primers were for: *(i) comt* ATGCCGGAGGCCCCGCCTCTG (forward) and GTCAGGGCCCTGCTTCGCTGC (reverse) as described in [103], *(ii) sequestosome (p62) CTGCCCAGACTACGACTTGTGT* (forward) and *TCAACTTCAATGCCCAGAGG* (reverse) and (iii) *gapdh CCACCCATGGCAAATTCCATGGCA* (forward) and *TCTAGACGGCAGGTCAGGTCCACC* (reverse). All PCR products were run on 2% agarose gels and stained with ethidium bromide. PCR was performed for 5-min at 95°C, then for *comt* 35 cycles of 30-sec at 95°C, 45-sec at 57°C and 45-sec at 72°C and for the *sequestosome* and *gapdh* 30 cycles of 30-sec at 95°C, 1-min at 52°C and 47-sec at 72°C with a final extension for all at 72°C for 5-min.

2.3.5. Subcellular Fractionation - After treatment for

24h, SK-N-SH cells in 10cm dishes ($6x10^5$ cells/ml) were rinsed twice with PBS. Cells were harvested by gently scraping into Hank's Balanced Salt Solution with 2mM EDTA and recovered by centrifugation at 500xg for 5-min. Subsequent homogenization, lysis and centrifugation steps were performed at 4°C. Following re-suspension in homogenization buffer (10mM HEPES, pH 7.4, 2mM EDTA, 250mM sucrose and 1.5mM PMSF) cells were homogenized by passing 25- to 30-times through a 22-gauge 1.5 needle/syringe. The subsequent homogenate was cleared of nuclear and cellular debris by centrifugation at 900xg for 15-min (S1 fraction). The S2 fraction (cytoplasm) was obtained by ultracentrifugation of S1 at 100,000xg for 2h in a Beckman TL-100 (Palo Alto, CA). The remaining pellet (P2, membrane fraction) was solubilized in 10mM HEPES, pH 7.4, 2mM EDTA, 0.5% Triton X-100 and 1.5mM PMSF for 12 h at 4°C. Protein concentrations of S2 and P2 fractions were determined using the bicinchoninic acid assay kit (Pierce, Rockf., IL).

2.3.6. Western Blotting - Total cell lysates as well as the S2 and P2 fractions were boiled for 5-min in Laemmli buffer and were analyzed by SDS-PAGE on 10% or 12% polyacrylamide gels followed by western blotting for detection of MB-COMT, S-COMT, sequestosome (p62) and COX-1

proteins with the respective antibodies. Antigens were visualized by a chemiluminescent horseradish peroxidase method with the ECL reagent.

2.3.7. Immunofluorescence - After treatment cell cultures were rinsed with PBS, fixed with ice cold methanol:acetone (1:1) for 10-min at -20°C and co-incubated with the antibodies listed in each figure. Slides were mounted with Vectashield medium containing DAPI (Vector Laboratories, Inc., Burlingame, CA). Cell staining was visualized with an OPTIPHOT-2 fluorescence microscope (NIKON, Melville, NY).

2.3.8. Quantification of S-adenosyl-L-methionine (SAM), dopamine (DA), 3,4-di-hydroxy-phenyl-acetic acid (DOPAC), 3-methoxytyramine (3MT) and homovanillic acid (HVA) - Following the treatment, cells were washed with ice-cold PBS, harvested in perchloric acid (0.4 N for SAM and 0.1N for dopamine and its metabolites) and centrifuged at 14,000xg for 15-min at 4°C, to ensure protein precipitation. Quantification of SAM was by high performance liquid chromatography (HPLC) as previously described [104]. Dopamine and its metabolites DOPAC, HVA, and 3MT were determined using HPLC with coulometric

electrochemical detection. The sample was separated on a reverse phase column (C18, 250 x 3 mm, 5 µ, Phenomenex, CA) by isocratic elution at a flow rate of 0.5 ml/min with a mobile phase consisting of potassium phosphate (0.05mM), octylsulfate (8.5mg/50 ml) and 14% methanol, adjusted to pH 2.65. Dopamine and its metabolites were detected using an electrochemical cell (model 5014B, ESA Inc, Chelmsford, MA) set to a potential of +400 mV. Data were acquired and processed using CoulArray for Windows software (ESA Inc, Chelmsford, MA). The PCA-precipitated proteins were neutralized with sodium hydroxide (0.2N) and the protein concentration of each sample was determined with the Bradford Assay (Bio-Rad Laboratories, Hercules, CA).

2.3.9. Cell Viability Assay - Cell viability was assessed with the 3-(4,5-dimethylthiazol-2-yl)-2,5-diphenyl tetrazolium bromide (MTT) assay as described in [105]. This assay assesses mitochondrial viability.

2.3.10. Statistical Analysis - Statistical significance was estimated using one-way ANOVA with the Tukey-Kramer multiple comparison test.

2.4. RESULTS

2.4.1. PGJ2 alters COMT expression - We carried out RT-PCR analysis with *comt* gene-specific primers to determine if PGJ2 alters *comt* gene expression in SK-N-SH cells. PGJ2 concentrations ranging between 15 and 25μM decreased *comt* mRNA levels in a concentration-dependent manner, reaching 0.1% of control levels at 25μM **(Figure 1)**. The levels of the control 18S rRNA were also decreased under these conditions, albeit to a lesser degree, declining to 33% of control. Not all genes are down-regulated in response to PGJ2-treatment. As shown in **Figure 1** and previously reported [106], PGJ2 concentrations ranging between 5 and 25μM caused a considerable elevation of *sequestosome* mRNA levels, reaching a maximum of 2.5-fold above control upon treatment with 20μM PGJ2 **(Figure 1)**. The *gapdh* mRNA levels did not change significantly under these conditions.

Expression of the human 30kDa membrane-bound and 25kDa soluble COMT polypeptides was detected by western blotting of the respective subcellular fractions **(Figure 2)**. MB-COMT rose to 1.9-fold above basal levels upon treatment with lower PGJ2 concentrations (5 to 15μM), while higher PGJ2 concentrations (20 and 25μM) decreased COMT-protein levels

to 87% of control. On the other hand, soluble COMT levels decreased in a PGJ2 concentration-dependent manner to 25% of control. A residual amount of MB-COMT, which paralleled MB-COMT detected in the membrane fraction, was also detected in the soluble fraction. To determine if the decrease in COMT protein levels was a general phenomenon associated with an overall decrease in protein synthesis we assessed the changes in the levels of another protein, i.e. sequestosome/p62 (Seq.), upon PGJ2-treatment. As previously shown [106], anti-Seq. immunoreactivity was detected only faintly in control cells. However, its protein levels increased in a PGJ2-dependent manner, rising to at least 24-fold above control in cells treated with 15μM PGJ2 **(Figure 2)**. The levels of cyclooxygenase 1 (COX-1), an ER membrane protein (reviewed in [107]) that is constitutively expressed in these cells, were not altered by the PGJ2-treatment.

2.4.2. PGJ2 induces the sequestration of COMT into large aggregates in human neuroblastoma SK-N-SH cells – In control cells, COMT exhibited a uniform reticular distribution that extended from the nuclear envelope out to the periphery of the cell with a characteristic ER morphology indicating that most of COMT is an ER resident

(Figure 3A and B). The distribution of COMT was altered by PGJ2 treatment. In cells treated for 24h with 5μM PJG2, COMT immunoreactivity appeared less diffuse throughout the cells and was more concentrated around the nuclei **(Figure 3C and D).** In cells treated with a higher PGJ2 concentration (15μM) COMT immunostaining emerged as a large perinuclear aggregate next to a nuclear indentation **(Figure 3E and F, *arrow*).**

2.4.3. PGJ2 induces the sequestration of COMT into large aggregates in rat (P2) primary cortical neurons - SK-N-SH cells are a human dopaminergic-like neuroblastoma cell line derived from peripheral tissue [101]. Notably, previous studies demonstrated catecholamine-induced toxicity in rat neocortical cultures [108]. We thus investigated if PGJ2 had the same effect on rat (P2) primary cortical neurons. Under control conditions, COMT-immunofluorescence was detected mostly in the cell body of the neurons with some staining apparent in cell processes as well **(Figure 4A).** The centrosome was also visible in the cell body upon immunostaining with the anti-γ-tubulin antibody **(Figure 4B, *arrow*).** After a 24h treatment with 15μM PGJ2, most of the COMT-immunoreactivity shifted to a single

large perinuclear aggregate **(Figure 4A′, *arrow*)** similar to the one detected in SK-N-SH cells. This COMT-aggregate was co-localized with the centrosome **(Figure 4B′ and 4C′, *arrows*)** suggesting an aggresome-like structure.

2.4.4. PGJ2 induces a decline in COMT activity – We assessed the activity of COMT, since its PGJ2-induced decline in expression and accumulation in large perinuclear aggregates was likely to impair its activity. COMT catalyzes the O-methylation of endogenous catecholamines (dopamine, norepinephrine and epinephrine) and other catechols (reviewed in [95]). S-adenosyl-L-methionine (SAM) is the principal biological methyl donor for COMT-catalyzed reactions. Thus intracellular levels of SAM are tied to COMT activity.

Based on this reasoning, we assessed changes in COMT activity by measuring SAM levels in SK-N-SH cells incubated for 24h with different concentrations of PGJ2 **(Figure 5A)**. Under basal conditions, SK-N-SH cells maintained a SAM concentration of 618.2 nmol/g of protein. After incubations for 24h with increasing concentrations of PGJ2, SAM levels were elevated to a maximum of 2 μmol/g of protein, a three-fold increase over basal levels. This increase in the

intracellular SAM concentration is likely to reflect a decline in COMT activity induced by PGJ2.

Dopamine is catabolized to its final metabolite HVA (homovanillic acid) through two metabolic pathways: 1) it is ***N***-oxidized by monoamine oxidase (MAO) to form DOPAC (3,4-dihydroxy-phenyl-acetic acid) which is then converted to HVA by COMT; and 2) it is ***O***-methylated by COMT to form 3MT (3-methoxytyramine), which is then converted to HVA by MAO **(Figure 5B, *insert*)**. To further assess COMT activity we compared the intracellular levels of dopamine and its metabolites in cells treated for 24h with 100μM of dopamine alone, or with 15μM PGJ2 six hours prior to the addition of 100μM dopamine. Dopamine was previously shown to enter SK-N-SH cells through the norepinephrine transporter [109]. Following treatment, intracellular levels of dopamine were equivalent in both groups of cells **(Figure 5B)**. Notably, in cells treated with PGJ2 and dopamine, DOPAC levels were two-fold higher than in cells treated with dopamine alone **(Figure 5B)** indicating a reduction in COMT activity. In cells treated with dopamine and PGJ2 the levels of 3MT, another dopamine metabolite, were not significantly lower ($p>0.05$) than in cells treated with dopamine alone

(Figure 5B). In these cells, conversion of dopamine to 3MT seems not to be the preferred pathway, as the concentration of this dopamine metabolite is low even in the absence of PGJ2. Surprisingly, the levels of HVA, a major catecholamine end product, were equivalent under both cell treatments.

2.4.5 PGJ2 exacerbates dopamine cytotoxicity – Dopamine decreases the viability of SK-N-SH cells in a concentration-dependent manner **(Figure 6, *open circles*).** Dopamine toxicity was significantly potentiated by pre-incubations with 5 or 15μM PGJ2 **(Figure 6, *solid squares and circles*, respectively).** These data suggest that COMT impairment by PGJ2 may contribute to the stability of dopamine and/or its metabolites, thereby increasing their intracellular levels and cytotoxicity.

2.5. DISCUSSION

We established that PGJ2-treatment resulted in a decline in COMT mRNA and protein levels in human dopaminergic-like neuroblastoma SK-N-SH cells. The *comt* gene encodes for both the membrane and soluble forms of COMT (reviewed in [95]). The majority of human tissues

contain both *comt* transcripts. However, soluble-COMT dominates by a factor of three or more in most human tissues, whereas membrane-COMT comprises 70% of total COMT in the human brain (reviewed in [110]). The variability in human *comt* gene expression suggests regulation by tissue-specific transcription factors. Notably, estradiol was shown to down-regulate the human *comt* gene transcription through an interaction of the estrogen receptor with response elements in the promoter region of the gene in a human breast carcinoma (MCF-7) cell line [111]. The mechanism by which PGJ2 induces changes in *comt* gene expression remains to be established.

We also show that upon PGJ2-treatment, COMT accumulates in large perinuclear aggregates in human SK-N-SH cells as well as in rat primary (P2) cortical neurons. As far as we know, ours is the first study to demonstrate that under stress conditions such as those induced by PGJ2, COMT is sequestered into large perinuclear aggregates. That these large aggregates may be aggresome-like structures is indicated by their co-localization with γ-tubulin, a centrosome/MTOC marker.

Prostaglandins of the J2 series were shown to induce an ER-stress response. Accordingly, 15d-PGJ2 triggered expression of the stress-inducible ER chaperone BiP [112].

Furthermore, 15d-PGJ2 activates CHOP, a transcription factor induced by ER-stresses [113]. Notably, studies with overexpressed MB-COMT in mammalian cell lines showed an absence of COMT bound to the plasma membrane. Instead, COMT was found to be anchored to the ER membrane with its catalytic site facing the cytoplasm [114]. Thus, the ER-stress response caused by prostaglandins of the J2 series is likely to be associated with the displacement of some ER proteins causing them to accumulate into large aggregates.

Our studies also establish that PGJ2-treatment leads to COMT impairment and exacerbates dopamine toxicity. COMT is one of the enzymes that metabolize dopamine. Thus COMT-impairment could affect dopamine levels. Parkinson's disease is characterized pathologically by the demise of dopaminergic neurons in the ***substantia nigra pars compacta*** (SNpc) (reviewed in [115]). These neurons appear to contain very low levels of COMT [116], although further studies are necessary to confirm this observation. One possible caveat to this finding is that the number of SNpc dopaminergic neurons decreases dramatically with age. Thus COMT levels in this region of the brain may therefore be underestimated (reviewed in [117]). If indeed SNpc dopaminergic neurons are low in COMT, this may partially explain why they are less protected from the oxidative damage induced by

dopamine. COMT-mediated methylation of dopamine is an important first-line detoxification pathway that renders this neurotoxic neurotransmitter and its catechol-containing precursor and/or metabolites biologically inactive and chemically inert (reviewed in [117]). If COMT-activity is further weakened in the SNpc neurons by conditions, such as inflammation and the ensuing production of prostaglandins of the J2 series, the intracellular concentrations of dopamine and/or its metabolites will even be more elevated. Thus, impairment of COMT-activity may be associated with an increase in the levels of oxyradicals and chemically reactive semi-quinone/quinone intermediates derived from dopamine oxidation, leading to oxidative stress and possible neuronal damage [118]. Notably, the COMT-inhibitor dinitrocatechol was shown to completely abolish the protective effect of methionine, dimethionine or SAM against L-dopa toxicity [119]. These results support the notion that COMT inhibition may aggravate or unmask L-dopa neurotoxicity.

We propose that through the production of prostaglandins of the J2 series, pro-inflammatory conditions may inhibit important cellular pathways involved in neuronal homeostasis. These prostanoids were shown to induce oxidative stress [42], disrupt the

ubiquitin/proteasome pathway [43;44], up-regulate COX-2 [33] and induce apoptosis [45]. We now demonstrate that PGJ2 impairs COMT activity. In conclusion, all of these PGJ2-effects are potential risk factors that may contribute to the demise of neuronal cells that occurs in neurodegeneration.

CHAPTER III

AGGREGATES OF UBIQUITINATED PROTEINS INDUCED BY PROSTAGLANDIN J2 ARE ASSOCIATED WITH CYTOSKELETON/ER COLLAPSE

Kenyon D. Ogburn and Maria E. Figueiredo-Pereira

From the Department of Biological Sciences, Hunter College of City University of New York, New York, New York 10021

3.1. ABSTRACT

Many neurodegenerative disorders, such as Parkinson's disease, exhibit inclusion bodies containing ubiquitinated proteins and signs of inflammation in the affected areas. The mechanisms implicated in the aggregation of ubiquitinated proteins into inclusion bodies remain elusive. We report that prostaglandin J2 (PGJ2), which is an endogenous product of inflammation, disrupts the cytoskeleton in neuronal cells. Furthermore, we show that PGJ2 perturbs microtubule polymerization *in vitro* and decreases the number of free sulfhydryl groups on tubulin cysteines. A direct effect of PGJ2 on actin was not so apparent, although the structure of actin filaments was perturbed in cells treated with PGJ2. This prostanoid triggered the collapse of the ER and induced the formation of protein aggregates shown to contain ubiquitinated proteins, α-synuclein, calnexin and catechol-*O*-methyltransferase (COMT). Moreover, upon PGJ2-treatment, most of the ubiquitinated proteins accumulated as detergent/salt-insoluble aggregates.

Our data support a mechanism by which, upon PGJ2-treatment, cytoskeleton/ER collapse leads to the accumulation of ubiquitinated proteins into insoluble aggregates. The co-localization of ubiquitinated proteins

with ER residents and other potentially neighboring proteins in the protein aggregates coincides with the collapse of the microtubule and ER networks. These events triggered by a product of inflammation may be common to other compounds that disrupt microtubules and induce protein aggregation, such as MPP^+ and rotenone, found to be associated with neurodegeneration.

3.2. INTRODUCTION

Protein aggregates containing ubiquitinated proteins are detected in a variety of degenerative diseases. These diseases range from neurological disorders, such as Alzheimer's disease, Parkinson's disease, amyotrophic lateral sclerosis and Huntington's disease, to liver diseases, such as Wilson's disease and alcoholic hepatitis, to name a few [2]. Whether these protein aggregates are pathogenic or represent a coping mechanism to prolong survival of the affected cells, including neurons and hepatocytes, is a hotly debated issue [120]. The protein aggregates, however, are indicative of a malfunction of the normal process of protein turnover since they are not prevalent in healthy cells.

Most of these protein aggregates are detectable with antibodies that react with ubiquitinated proteins but their

major structural components vary from cell type to cell type. For example, tau proteins are found in cortical neurofibrillary tangles, α-synuclein in dopaminergic Lewy bodies and huntingtin in intranuclear inclusions of striatal projection neurons (reviewed in [3]). Full characterization of the components and mechanisms leading to the formation of these protein aggregates is lacking.

Notably, most of the diseases associated with the accumulation of ubiquitinated proteins in intracellular inclusions also exhibit signs of inflammation in the respective damaged areas (reviewed in [5]). Our studies focus on one of the products of inflammation, prostaglandin J2 (PGJ2), because recent reports indicate that these cyclopentenone prostaglandins may play an important role in neurodegeneration. For example, the levels of 15d-PGJ2, a PGJ2 metabolite, were found to be elevated in spinal cord motor neurons of patients with amyotrophic lateral sclerosis [45]. Furthermore, J2 prostaglandins were shown to be neurotoxic and pro-oxidant agents [42;121], to up-regulate the expression of cyclooxygenase-2 [33], to inhibit ubiquitin isopeptidase activity [43] as well as UCH-L1 and UCH-L3 [44], and to induce the accumulation of ubiquitinated proteins [42] and neuronal apoptosis [45]. All of these events are associated with neurodegeneration.

We recently demonstrated that J2 prostaglandins induce the accumulation of ubiquitinated proteins into distinct aggregates in neuronal cells [44]. To understand the mechanisms leading to the formation of these protein aggregates and to identify some of their components, we investigated the effects of PGJ2 on human neuroblastoma SK-N-SH cells. Herein, we show that PGJ2 damages the cytoskeletal structure. The ensuing microtubule disruption and ER collapse coincides with the formation of protein aggregates co-localized with the microtubule organizing center (MTOC). In addition to ubiquitinated proteins, the PGJ2-induced protein aggregates contain calnexin, catechol-*O*-methyltransferase (COMT) and α-synuclein. Thus, products of inflammation, such as PGJ2, destabilize the microtubule network resulting in collapse of the ER and trigger the formation of protein aggregates containing ubiquitinated proteins. Most of the ubiquitinated proteins accumulate as insoluble aggregates. In conclusion, disruption of the microtubule and ER networks in conjunction with the accumulation of ubiquitinated proteins, both caused by PGJ2, may represent mechanisms shared by other inducers of protein aggregation associated with neurodegeneration.

3.3. MATERIALS AND METHODS

3.3.1. Materials - PGJ2 was from Cayman Chemical (Ann Arbor, MI). 3-(4,5-Dimethylthiazol-2-yl)-2,5-diphenyl-tetrazolium bromide (MTT), colchicine and brefeldin A were from Sigma (St. Louis, MO). Kits to assess tubulin and actin polymerization were from Cytoskeleton, Inc. (Denver, CO). The following primary antibodies were used: rabbit polyclonal anti-COMT (1:500, from Chemicon Int., Temecula, CA), goat polyclonal anti-calnexin (C-20, 1:40) from Santa Cruz Biotechnology, Inc. (Santa Cruz, CA), mouse monoclonal anti-actin (1:200, clone AC-20) and mouse monoclonal anti-γ-tubulin (1:200, clone GTU-88) from Sigma (St. Louis, MO), rabbit polyclonal anti-α-tubulin (1:200) from Abcam Inc., (Cambridge, MA), mouse monoclonal anti-α-synuclein (1:200) from Zymed Lab. Inc. (San Francisco, CA), mouse monoclonal and rabbit polyclonal anti-ubiquitinated proteins antibodies (1:250) from Chemicon Int. (Temecula, CA) and Dako Cytomation (Carpinteria, CA), respectively. The respective secondary antibodies with fluorophores (1:50) were from Jackson ImmunoResearch Laboratories, Inc. (West Grove, PA).

3.3.2. Cell cultures - SK-N-SH cells are a human neuroblastoma cell line derived from peripheral tissue [101]. The cells were maintained as described in [33] and were obtained from ATCC.

3.3.3. Cell Treatments - SK-N-SH cell cultures were treated for 24h with vehicle (DMSO) or with increasing concentrations of PGJ2 in DMSO added directly to serum-containing medium. The final DMSO concentration in the medium was 0.5%. At the end of the incubation, all cultures were washed twice with phosphate buffered saline (PBS) and processed for the different assays as described below. Cell washes removed unattached cells, therefore subsequent assays were performed on adherent cells only.

3.3.4. Immunofluorescence - After treatment SK-N-SH cells were rinsed with PBS, fixed with ice cold methanol:acetone (1:1) for 10-min at -20^{o}C and co-incubated with the antibodies listed in each figure. Slides were mounted with Vectashield medium containing DAPI (Vector Laboratories, Inc., Burlingame, CA). Cell staining was visualized with an OPTIPHOT-2 fluorescence microscope (NIKON, Melville, NY).

3.3.5. In vitro tubulin and actin polymerization - Standard tubulin and actin polymerization assays were performed with kits from Cytoskeleton Inc., (Denver, CO) following the manufacturer's recommendations. Tubulin polymerization was assessed at 340nm every 60-sec with a temperature-regulated Power Wave 200™ microplate scanning spectrophotometer, Bio-Tek Instruments, Inc. (Winooski, VT). Actin polymerization was assessed at 365/407nm every 60-sec with a 650-10S Fluorescence Spectrophotometer equipped with a 150 Xenon Power Supply, Perkin Elmer (Wellesley, MA). Data were analyzed with KC4 Kineticalc for Windows, Bio-Tek Instruments, Inc.

3.3.6. DTNB assay for free tubulin sulfhydryl groups - Tubulin (3µg/µl, 50µl) in general tubulin buffer with 1mM GTP was incubated under basal conditions with 5µl of general tubulin buffer alone or containing DMSO (1.5%), PGJ2 (273µM or 545µM) or PGE2 (545µM) for 90-min, with gentle rocking at 37°C. Free sulfhydryl groups were assessed with 5,5'-Dithio-bis(2-nitrobenzoic acid) (DTNB) essentially as described in [122]. A standard curve with L-cysteine (10-20nmol) was used to calculate the free sulfhydryls in the tubulin samples.

3.3.7. Subcellular Fractionation - After treatment for 24h, SK-N-SH cells in 10cm dishes (4.5 x 10^5 cells/ml) were rinsed twice with PBS. Cells were harvested by gently scraping into ice-cold homogenization buffer [15mM Tris-HCl, pH 7.6, 1mM DTT, 0.25M sucrose, 1mM $MgCl_2$, 2.5mM EDTA, 2.5mM EGTA and protease inhibitor cocktail (Sigma, St. Louis, MO) supplemented with 1mM Na_3VO_4, 25mM NaF and 2mM sodium pyrophosphate]. All subsequent steps were carried out at 4°C. Homogenization and subcellular fractionation were performed as described in [123]. Briefly, samples were homogenized with a Dounce homogenizer (30-strokes) followed by a 10-min centrifugation at 1,000xg to obtain the crude nuclear pellet (P1) and supernatant fraction (S1). S1 was centrifuged at 10,000xg to collect the pellet (P2). The S2 supernatant was further centrifuged at 162,000xg for 1h in a Beckman TL-100 (Palo Alto, CA) to collect the cytosolic fraction (S3) and the microsomal pellet (P3). The P2 pellet was resuspended in homogenization buffer containing 1% Triton X-100 (TX) and 400mM KCl, sonicated five times for 5-sec each, washed on a shaker for 1h followed by a 10-min centrifugation at 20,000xg to obtain the TX-insoluble and TX-soluble fractions. The P1 and TX-insoluble pellets were re-suspended in denaturing buffer (10mM Tris-HCl, pH 7.3, 1% SDS and 1mM Na_3VO_4).

3.3.8. Western Blotting - Western blot analysis was carried out by SDS-PAGE on 8% polyacrylamide gels. Samples were boiled for 5-min in Laemmli buffer and loaded onto the gel (5µg of protein/lane). Following electrophoresis, proteins were transferred to an Immobilon-P membrane (Millipore, Bedford, MA). The membrane was probed with an antibody that reacts with poly-ubiquitinated proteins (1:1,500, from Dako Cytomation, Carpinteria, CA). Antigens were visualized by a chemiluminescent horseradish peroxidase method with the ECL reagent.

3.3.9. Protein concentration - was determined with the bicinchoninic acid assay kit (Pierce, Rockford, IL) or the Bradford Assay (Bio-Rad, Hercules, CA).

3.4. RESULTS

3.4.1. PGJ2 disrupts the cytoskeletal structure - To determine the effect of PGJ2 on the cytoskeleton we visualized two of its components, namely microtubules and actin filaments, by immunofluorescence analysis with anti-α-tubulin and anti-actin antibodies, respectively. We chose to treat cells with 15µM PGJ2 for 24h because in our

previous studies, these conditions clearly induced both accumulation and aggregation of ubiquitinated proteins as well as neuronal cell death [44].

In the absence of PGJ2, microtubules and actin filaments were intact, straight and oriented parallel to the longest axis of the SK-N-SH cells **(Figure 7, A, B & E).** Upon treatment for 24h with 15μM PGJ2, the appearance of the microtubule network and actin filaments was altered. The microtubules were fragmented and displayed a circular arrangement surrounding the nucleus **(Figure 7, C and F)** and the actin filaments exhibited an amorphous pattern **(Figure 7, D).** The shape of the cell complemented the change observed for the microtubule network. Control cells were elongated **(Figure 7, A, B & E)** while PGJ2-treated cells displayed a round to square shape **(Figure 7, C, D & F).**

The alterations in microtubule appearance elicited by PGJ2 suggest that this product of inflammation affects microtubule polymerization. We thus investigated the effect of PGJ2 on the ***in vitro*** polymerization of highly purified (>99%) bovine brain tubulin at pH 6.9 and 37°C, as described under "Materials and Methods". The effect of PGJ2 on microtubule assembly was determined as a function of time with a turbidimetric assay. The ***in vitro*** microtubule

polymerization assay requires high tubulin concentrations (3mg/ml or 54.5μM) for turbidity assessment, thus we increased the PGJ2 concentrations in the ***in vitro*** assay, accordingly. Other compounds found to oxidize tubulin sulfhydryls, such as peroxynitrite, were tested at similar concentrations [122].

Standard polymerization reactions in the absence of drug or solvent (***open squares, black***) or in the presence of 1.5% DMSO (prostaglandin solvent, ***open squares, blue***), or 545μM PGE2 (***solid squares, blue***), or 273μM and 545μM PGJ2 (***open and solid squares, red, respectively***) are shown in **Figure 8A**. The curves represent the average of two experiments. The Vmax for each curve is listed in **Figure 8B**. Tubulin polymerizes with a Vmax of approximately 5.5 milli OD units per minute (mOD/min) in the general tubulin buffer (GTB) plus GTP, indicating a low efficiency of polymerization under these conditions. DMSO alone (1.5% final concentration) eliminates the nucleation phase of polymerization and enhances the Vmax of the growth (elongation) phase by approximately four-fold. Others have reported that DMSO induces self-assembly of tubulin [124]. Although the mechanism is not well characterized, it was suggested that solvents such as DMSO alter the H_2O structure around the tubulin dimers lowering the free energy of

polymerization.

In the presence of PGJ2 (in 1.5% DMSO) tubulin polymerization was hindered as depicted by a significant decrease in Vmax and in levels of assembled microtubules when compared to DMSO alone **(Figure 8A and B)**. The Vmax was lowered by 28% and 43% by 273μM and 545μM PGJ2, respectively **(Figure 8B)**. PGE2, a prostaglandin that does not cause aggregation of ubiquitinated proteins, did not affect microtubule polymerization (**Figure 8A and B)**.

Prostaglandins of the J2 series are unique among the prostaglandin family as they contain α,β-unsaturated carbonyl groups in their cyclopentenone ring [37]. One of these prostaglandins, 15-deoxy-$\Delta^{12,14}$-prostaglandin J2, was recently shown to induce cysteine-targeted protein oxidation in SH-SY5Y cells [125]. Furthermore, tubulin was one of the proteins that was identified as being *S*-oxidized in these cells. Microtubules are composed of the heterodimeric protein tubulin that contains 20 cysteines: 12 in the α- and 8 in the β-subunit [126;127]. We thus reasoned that PGJ2 may hinder microtubule polymerization by inducing the *S*-oxidation of free sulfhydryl groups in tubulin. To test our hypothesis, we assessed the levels of free sulfhydryl groups in purified tubulin incubated in the

absence and presence of PGJ2, using 5,5'-Dithio-bis(2-nitrobenzoic acid) (DTNB). This reagent forms a colored product measurable at 412nm when it reacts with free sulfhydryl groups. **Figure 8C** depicts the decrease in the levels of DTNB-reactive sulfhydryls in tubulin elicited by PGJ2-treatment. A 22% and 35% drop in free sulfhydryls was observed when tubulin was treated with 273μM and 545μM PGJ2, respectively. The decrease in free tubulin sulfhydryl groups induced by PGJ2 correlated well with its inhibition of microtubule polymerization **(Figure 8A-C)**. No decline in free tubulin sulfhydryl groups was detected in the presence of 545μM PGE2, a prostaglandin that does not contain α,β-unsaturated carbonyl groups.

PGJ2 also disrupted the structure of actin microfilaments in SK-N-SH cells. Thus we assessed the effect of PGJ2 on ***in vitro*** actin polymerization by pyrene fluorescent enhancement as described under "Materials and Methods". DMSO alone (1.5% final concentration) slightly enhanced the Vmax of actin polymerization by approximately 1.4-fold, when compared to general actin buffer (GAB) **(Figure 9B)**. However, the levels of polymerized actin were not altered by DMSO **(Figure 9A)**. In the presence of PGJ2 or PGE2 the Vmax and polymerized actin levels were equivalent to the ones observed for DMSO and GAB **(Figure 9A and B)**. We

thus conclude that PGJ2 failed to directly affect actin polymerization in this *in vitro* assay.

3.4.2. PGJ2 induces the collapse of the ER and formation of large protein aggregates - It is well established that the morphology and stability of the ER are maintained by its attachment to microtubules [128;129]. Furthermore, microtubule disruption causes the ER to retract towards the nucleus [128;129]. Since we observed that PGJ2 disrupts microtubule integrity, we investigated the effect of PGJ2 on ER morphology assessed by immunofluorescence analysis with an anti-calnexin antibody. Calnexin is a membrane-bound ER resident protein and under control conditions, it exhibits a uniform reticular distribution that extends from the nuclear envelope out to the periphery of the cell with a characteristic ER morphology **(Figure 10B)**. Similarly, immunofluorescence staining for COMT, an enzyme that catalyzes the metabolism of catecholamines including dopamine, revealed its predominant ER localization **(Figure 10C)**.

The distribution of calnexin and COMT was altered by PGJ2 treatment. In cells treated for 24h with 5μM PJG2, calnexin and COMT immunoreactivity appeared less diffuse throughout the cells and was more concentrated around the

nuclei **(Figure 10E and F)**. In cells treated with a higher PGJ2 concentration (15μM) calnexin and COMT immunostaining emerged as a large perinuclear aggregate next to a nuclear indentation **(Figure 10H and I, *arrows*)**. This pattern of immunostaining suggests that the ER collapsed into a large perinuclear aggregate.

The large perinuclear aggregate detected in PGJ2-treated cells resembles aggresomes, first described by Kopito's group [130]. Aggresomes are thought to be deposition sites for ubiquitinated proteins that escape degradation by the ubiquitin/proteasome pathway. In addition, aggresomes were shown to be co-localized with centrosome/MTOC markers (reviewed in [131]). We also found that the large perinuclear aggregate detected with the anti-calnexin **(Figure 10H)** and anti-COMT **(Figure 10I)** antibodies in PGJ2-treated cells was co-localized with γ-tubulin, a centrosome marker **(Figure 11E-H)**. Under control conditions **(Figure 11A-D)**, COMT immunostaining was distributed throughout the cells and was not concentrated around the centrosome/MTOC.

3.4.3. Formation of protein aggregates in PGJ2-treated cells is time-dependent and coincides with microtubule collapse – Since calnexin and COMT have similar subcellular

distributions, we focused our studies on COMT changes, since the activity of this enzyme may be relevant to neurodegeneration [117]. No microtubule alterations or protein aggregates were detected by immunofluorescence analysis after 4h of treatment with 15μM PGJ2 **(Figure 12A and B)**. Eight hours after PGJ2-treatment a slight indication of microtubule disruption, as well as COMT-concentration around the nuclei, were noticeable **(Figure 12C and D)**. At 16h post-treatment **(Figure 12E and F)**, the microtubules appeared already fragmented and formed a circular network around the nuclei; COMT immunoreactivity emerged as a large aggregate co-localized with the centrosome depicted by γ-tubulin immunostaining. These changes observed after 16h of treatment with 15μM PGJ2 were similar to the ones detected upon 24h of treatment **(Figure 12G and H)**.

3.4.4. Biochemical analysis of PGJ2-induced protein aggregation – The protein aggregation and microtubule disruption patterns induced by PGJ2 were mimicked by treating cells with colchicine, a drug that disrupts the microtubule/ER network. Large perinuclear aggregates containing ubiquitinated proteins **(Figure 13A, *arrow*)** and

calnexin **(Figure 13B, *arrow*)** as well as microtubule collapse **(Figure 13C)** were observed in colchicine-treated cells. Perturbation of Golgi function by treating cells with brefeldin A did not duplicate the effect of PGJ2-treatment on protein aggregation. Ubiquitinated proteins where detected mostly in the nuclei and the perinuclear/ER area **(Figure 13D and G).** As expected, calnexin staining was very low in the nuclei of brefeldin A-treated cells, since calnexin is an ER resident protein **(Figure 13E).** Microtubule structure was also disrupted by treatment with brefeldin A but not to the extent observed with colchicine or PGJ2 **[compare Fig. 13C (colchicine) and H (brefeldin A) with I (control)].**

Western blot analysis of lysates from SK-N-SH cells treated with PGJ2, brefeldin A or colchicine for 4, 8, 16 and 24h showed that PGJ2 specifically induced the greatest accumulation of ubiquitinated proteins at 16h. However, this effect was not observed with cells treated with brefeldin A and colchicine **(Figure 14).** Stripping and re-probing the blots with a COX-1 antibody demonstrated no apparent change in its levels. These results suggest that the accumulation of ubiquitinated proteins at 16h likely coincides with the formation of the MTOC-localized COMT aggregate, as seen in **Figure 12F**, ***arrow***.

To characterize the aggregates of ubiquitinated proteins that accumulate upon PGJ2-treatment we performed subcellular fractionation followed by western blot analysis for ubiquitinated proteins. As shown in **Figure 15**, upon PGJ2-treatment most ubiquitinated proteins were detected in the Triton X/salt-insoluble fraction, suggesting that they occur as insoluble aggregates. However, some ubiquitinated proteins were also detected in the crude nuclear pellet as well as microsomal fraction.

3.4.5. The protein aggregates induced by PGJ2 contain ubiquitinated proteins, α-synuclein, COMT and calnexin - Under control conditions, only low levels of ubiquitinated proteins were detected and they exhibited a diffuse distribution throughout the cytoplasm and nucleus **(Figure 16B and J)**. Most of the ubiquitinated proteins in PGJ2-treated cells were consistently concentrated in a single large, perinuclear aggregate **(Figure 16F and N, *arrows*)**. Low levels of ubiquitinated protein immunoreactivity were also detected in small punctuated aggregates scattered throughout the cells.

We established that in PGJ2-treated cells, the large perinuclear aggregate contained high levels of α-synuclein **(Figure 16G, *arrow*)**. The latter is one of the major

components of dopaminergic Lewy bodies detected in the ***substantia nigra*** of Parkinson's disease patients. Under control conditions, α-synuclein immunoreactivity exhibited a punctated appearance more or less evenly distributed throughout the cell with very low levels in the nucleus, if any **(Figure 16C)**.

In PGJ2-treated cells, most of the ubiquitinated proteins are co-localized in the large perinuclear aggregate with α-synuclein **(Figure 16H)** and COMT **(Figure 16P)**. As shown in **Figure 10**, the distribution of COMT matched that of calnexin in the protein aggregates. Therefore, it appears that the microtubule and ER collapse triggered by PGJ2-treatment coincides with the redistribution of these three proteins, i.e. calnexin, COMT and α-synuclein, as well as ubiquitinated proteins into the large protein aggregates.

3.5. DISCUSSION

The mechanisms implicated in the formation of aggregates containing ubiquitinated proteins detected in neurodegenerative disorders remain elusive. We recently demonstrated that J2 prostaglandins, which are endogenous

products of inflammation, trigger the aggregation of ubiquitinated proteins [44]. However, the mechanisms leading to this protein aggregation and the components of the distinct protein deposits were not defined.

To elucidate the mechanism of protein aggregation induced by PGJ2, we investigated its effect on the cytoskeletal structure of human neuroblastoma SK-N-SH cells. Herein, we show that PGJ2 disrupts the structural integrity of microtubules and actin microfilaments in the SK-N-SH cells. Furthermore, we established that PGJ2 perturbs the ***in vitro*** polymerization of highly purified tubulin from bovine brain. Notably, the reactive oxygen species peroxynitrite was shown to oxidize tubulin sulfhydryls and impair microtubule polymerization [122]. Furthermore, a product of lipid peroxidation, 4-hydroxynonenal, covalently modifies proteins by forming Michael adducts. Interestingly, 4-hydroxynonenal also disrupts neuronal microtubules and modifies cellular tubulin [133]. We established that PGJ2 has similar effects. It disrupts microtubule integrity, impairs microtubule polymerization and decreases the number of free sulfhydryls on tubulin cysteines. The unsaturated carbonyls of J2 prostaglandins are known to covalently modify free cysteines in proteins by the Michael’s addition reaction

[37]. Moreover, J2 prostaglandins increase the intracellular levels of products of lipid peroxidation, such as 4-hydroxynonenal and acrolein [42]. Thus the disruption of microtubule integrity detected in PGJ2-treated cells may be caused by the formation of complexes between PGJ2 (or its metabolites) and tubulin and/or by a more indirect mechanism mediated by, for example, formation of 4-hydroxynonenal.

We observed that actin filaments were disrupted in cells treated with PGJ2. However, we could not detect a direct effect of this prostanoid on actin, as assessed by an ***in vitro*** actin polymerization assay involving pyrene fluorescent enhancement. Unlike the heterodimeric protein tubulin that contains 20 cysteines (12 in the α- and 8 in the β-subunit), actin contains only five cysteines. From these, only one (Cys374) seems to be susceptible to Michael adduction [134]. It is possible that the ***in vitro*** assay is not sensitive enough to detected polymerization changes caused by only one cysteine per actin molecule. Alternatively, PGJ2 may have no direct effect on actin. Instead, the effect of PGJ2 on microtubules observed in SK-N-SH cells may trigger a cascade of cellular responses that will then perturb microfilament assembly.

It is well established that disruption of the microtubule network leads to ER collapse, thus forming an aggregate of membranes around the nucleus (reviewed in [129]). Our studies show that disruption of the microtubule structure induced by PGJ2-treatment coincides with ER collapse into a large perinuclear aggregate that is co-localized with a centrosome/MTOC marker. As far as we know, ours is the first study showing that microtubule/ER collapse coincides with the formation of protein aggregates in cells treated with PGJ2. We observed a similar effect in rat primary cortical neurons treated with PGJ2 [135].

Aggresomes induced by overexpression of several mutant proteins, such as CFTR, or by proteasome inhibitors, were previously reported to be surrounded by but not co-localized with the ER [130;136]. The PGJ2-induced large aggregates share some of the aggresome properties, such as being co-localized with the centrosome/MTOC and containing detergent/salt-insoluble proteins. However, aggresomes are cytoplasmic and their formation requires an intact cytoskeleton.

In contrast, PGJ2-induced aggregates are associated with the collapse of the microtubule/ER network and their formation can be mimicked by treating cells with colchicine, a drug that like PGJ2, disrupts microtubules.

Brefeldin A, which interferes with Golgi function, did not mimic the effect of PGJ2 on protein aggregation. In fact, ubiquitinated proteins were trapped in the nucleus and perinuclear area of brefeldin A-treated cells. Moreover, the effect of PGJ2 on the accumulation of these ubiquitinated proteins appears to be both specific and time-dependent, as brefeldin A and colchicine did not induce significant ubiquitinated protein accumulation over time. Taken together, these results demonstrate that PGJ2-induced aggregates are subcellular structures that are different from aggresomes.

The protein aggregates induced by treatment with PGJ2 contained not only ubiquitinated proteins, but also α-synuclein, calnexin and COMT. The two latter proteins, i.e. calnexin and COMT, have not yet been identified as components of protein aggregates. Based on these data, we propose a model in which cytoskeleton/ER collapse induced by PGJ2 is likely to displace many intracellular proteins causing them to co-localize in protein aggregates. These protein aggregates are likely to include an unspecific collection of proteins depending on their proximity to the collapsing microtubule and ER networks, levels of expression, aggregation susceptibility and cell type.

Overall, our data support the notion that cytoskeleton/ER collapse induced by an endogenous product of inflammation, PGJ2, may be closely associated with the neurodegenerative process. Interestingly, recent studies have demonstrated that parkin binds strongly to and stabilizes microtubules [137;138]. It was suggested that since parkin is anchored to and stabilizes microtubules and that many of its substrates are transmembrane or membrane-associated proteins, parkin may be optimally suited to meet the challenge of perturbed protein degradation in the ER [138]. Furthermore, α-synuclein appears to be a microtubule-associated protein, in this aspect resembling tau protein. Wild type α-synuclein was shown to induce the ***in vitro*** polymerization of tubulin into microtubules, while the two mutant forms of α-synuclein associated with Parkinson's disease do not [139]. Moreover, toxins such as MPP^+ and rotenone, which induce Parkinson's disease symptoms in animal models, strongly hinder microtubule polymerization [140-142]. The findings from all of these studies seem to converge on the premise that preserving microtubule integrity is vital to neuronal homeostasis. Disruption of the microtubule network will most likely cause defects in axonal transport, a mechanism that seems

to be common to many neurodegenerative disorders (reviewed in [143]).

Physiological concentrations of prostaglandins in body fluids are found to be in the pico-nanomolar range [92]. However, their levels rise considerably under pathological conditions such as hyperthermia, infection and inflammation, reaching the micromolar range at the site of damage [93]. The PGJ2 concentrations tested in our studies reflect, most likely, endogenous PGJ2 concentrations produced under pathological conditions. The rise in neurotoxic prostaglandins, such as J2 prostaglandins, in the CNS might be an integral component of the cellular response to an insult evoked by physical, chemical or microbial stimuli. However, the resulting neuronal cell death may have devastating effects as, in the vast majority of cases, neurons lost to disease cannot be replaced. It is thus critical that we learn more about the effects of neuroinflammation and its products, to be able to design therapies that will prevent endangered neurons from dying.

CHAPTER IV

PROSTAGLANDIN J2 ALTERS 26S PROTEASOME ASSEMBLY IN HUMAN NEUROBLASTOMA CELLS

4.1. ABSTRACT

Ubiquitinated proteins are degraded by the 26S proteasome, shown here to be the most active proteasomal form in SK-N-SH cells. We also demonstrate that PGJ2 impairs 26S proteasome assembly, which is an ATP-dependent process. Interestingly, PGJ2 is known to perturb mitochondrial function, which could be critical to the observed 26S proteasome disassembly implying a crosstalk between mitochondrial and proteasomal impairment.

In conclusion neurotoxic products of inflammation, such as PGJ2, may play a role in neurodegenerative disorders associated with the aggregation of ubiquitinated proteins by impairing 26S proteasome activity and inducing a chain of events that culminates in neuronal cell death.

4.2. INTRODUCTION

Unlike most other classes of eicosanoids, J2 prostaglandins are characterized by the presence of a cyclopentenone ring with α,β-unsaturated carbonyl groups that are able to form Michael adducts with nucleophiles such as free sulfhydryls in cysteine residues of glutathione and cellular proteins [37]. That J2 prostaglandins may play a role in neurodegeneration is supported by the finding that 15d-PGJ2 is elevated in spinal cord motor neurons of ALS

patients [45]. In addition, these prostaglandins induce apoptosis [144-146] and the accumulation and aggregation of polyubiquitinated proteins in neuronal cells [44].

To determine if PGJ2 affects the proteasome we investigated the effect of PGJ2 on proteasome activity by an in-gel assay. We observed that PGJ2 perturbs the assembly of the 26S proteasome. The chemical properties of J2 prostaglandins in conjunction with their pro-oxidant and ubiquitin/proteasome pathway disrupting effects render these cyclopentenone prostaglandins extremely neurotoxic and capable of inducing neuronal cell death (reviewed in [147]).

4.3. MATERIALS AND METHODS

4.3.1. MATERIALS – The proteasome inhibitor PSI [(N-benzyloxycarbonyl-Ile-Glu(O-t-butyl)-Ala-leucinal)] was obtained from Peptides International, Inc., Louisville, KY. The calpain/cathepsin inhibitor Z-LL-CHO (N-benzyloxycarbonyl-Leu-leucinal) was obtained from EMD Biosciences, San Diego, CA.

4.3.2. In-Gel Proteasome Activity and Detection – SK-N-SH cells treated for 24h with vehicle (DMSO) or PGJ2 (15μM and 20μM) were washed twice with PBS to remove

extracellular prostaglandins and were then harvested with the following buffer A: 50mM Tris-HCl, pH 7.4, 5mM $MgCl_2$, 5mM ATP (grade 1; Sigma), 1mM DTT and 10% glycerol. Following homogenization the protein content of the cleared supernatants (determined with the Bradford assay, BIO RAD) was adjusted to equal concentrations with buffer A. The cleared supernatants were resolved by non-denaturing PAGE using a modification of the method described in [148]. We used a four gel layer consisting of equal amounts, from the bottom up, of 6, 5, 4 and 3% polyacrylamide with Rhinohide™ polyacrylamide strengthener (Molecular Probes). Bromophenol blue was added to the protein samples prior to loading. Non-denaturing minigels were run at 125Volts for 2.5 hours. The gels were then incubated on a rocker for 30-min at 37°C with 10ml of 0.4mM Suc-LLVY-AMC in buffer B (buffer A modified to contain 1mM ATP only). Proteasome bands were visualized upon exposure to UV light (360nm) and were photographed with a NIKON Cool Pix 8700 camera with a 3-4219 fluorescent green filter (Peca Products, Inc.).

Proteins on the native gels were transferred (110mA) for 2h onto PVDF membranes. Western blot analyses were then carried-out sequentially for detection of the 26S and 20S proteasomes with anti-α4 subunit and anti-S8 subunit antibodies obtained from BIOMOL (Plymouth Meeting, PA). The

anti-α4 antibody reacts with a core particle subunit, therefore detects both the 26S and 20S proteasomes. The anti-S8 antibody reacts with a regulatory particle subunit thus only detecting 26S proteasomes. Antigens were visualized by a chemiluminescent horseradish peroxidase method with the ECL reagent.

4.3.3. 26S proteasome Activity in Cell Lysates - The chymotrypsin-like activity of the proteasome in cleared lysates obtained from SK-N-SH cells treated for 24h with vehicle only (DMSO) or PGJ2 (15μM), was assessed as described in [149]. To assure removal of extracellular prostaglandins the medium was aspirated and cells were washed twice with PBS before lysis. Cells were harvested in buffer A to preserve 26S proteasome assembly. Following homogenization protein concentration of cleared supernatants was normalized with buffer A. Proteasome chymotrypsin-like activity was assayed colorimetrically with the substrate Suc-LLVY-AMC as described in [149].

4.4. RESULTS

4.4.1. Inhibition of the activity of the 26S proteasome by PGJ2 involves proteasome disassembly - To address the effects of PGJ2 on the proteasome, we compared

proteasome activity and levels by non-denaturing gel electrophoresis of crude extracts from control and PGJ2-treated SK-N-SH cells.

In control cells, most of the proteasome activity assessed with the short substrate Suc-LLVY-AMC coincided with the 26S holoenzyme (not the 20S) form of the proteasome **(Figure 17, left panel)**. A concentration-dependent decrease in the chymotrypsin-like activity of 26S as well as 20S proteasomes was observed in cells treated with 15 and 20μM PGJ2.

Western blot analysis of the native gels probed with an antibody that reacts with the α4 subunit of the core particle revealed that the 26S and 20S proteasome levels are similar in control cells **(Figure 17, middle panel)**. However, an increase in 20S proteasome with a concomitant decrease in the 26S holoenzyme was observed upon treatment with PGJ2 **(Figure 17, middle panel)**. PGJ2 may thus alter the assembly state of 26S proteasome. This view was supported by the finding that stripping and reprobing the immunoblot with an antibody that reacts with the S8 subunit (an ATPase) of the 19S regulatory particle, showed a PGJ2 dose-dependent decline in 26S proteasome **(Figure 17, right panel)**. This finding confirms that PGJ2-treatment promotes disassembly of the 26S proteasome into free 20S core

particles. Free 19S particles were not detected.

4.4.2. Effect of PGJ2 on the chymotrypsin-like activity of cell lysates* (*These studies are a work in progress) - We assessed the chymotrypsin-like activity of crude cell lysates harvested in a buffer that preserves the assembled 26S proteasome. This buffer was the same used for analyzing cell lysates by non-denaturing gel electrophoresis. Treatment of SK-N-SH cells with 15μM PGJ2 for 24h did not alter the chymotrypsin-like activity of the cell lysates.

To address the discrepancy between the results obtained with the in-gel and total lysate activity assays we compared the effects of a proteasome (PSI) and a calpain/cathepsin inhibitor on cell lysate activity, because the substrate Suc-LLVY-AMC can also be cleaved by calpains. Indeed, we found that both the proteasome inhibitor PSI and the calpain inhibitor Z-LL-CHO inhibited the Suc-LLVY-AMC hydrolyzing activity of cell lysates. Therefore assessing changes in proteasome by measuring the chymotrypsin-like activity of total cell lysates with Suc-LLVY-AMC is misleading. Other proteases present in the total cell lysates can cleave the substrate.

The in-gel activity assay is therefore the preferred

method for assessing proteasome activity in cells, because native PAGE separates proteins according to charge and size. As far as we know, there are no other intracellular proteases that migrate on native PAGE with a pattern similar to that of the 26S and 20S proteasomes.

4.5. DISCUSSION

Recent studies demonstrated that treatment of SH-SY5Y cells with 15d-PGJ2 induced formation of 15d-PGJ2/proteasome conjugates [150] and oxidation of the S6 ATPase subunit of the 26S proteasome [151]. These modifications could contribute to decreased proteasome activity. The effect of PGJ2 on proteasome activity is controversial. While some studies show that J2 prostaglandins fail to inhibit proteasome activity in cells [43;44] others report the opposite, i.e. that J2 prostaglandins decrease proteasome activity [150]. This discrepancy could be due to the buffers used to harvest the cells. The different buffers may or may not preserve the assembly state of the 26S proteasome.

To address this issue we assessed proteasome activity by an in-gel assay in cells harvested with a buffer that preserves the assembly of the 26S proteasome. Our studies demonstrate that in control cells, the majority of the

proteasome chymotrypsin-like activity coincides with the 26S proteasome, suggesting that the free 20S core particle is nearly inactive. A similar phenomenon was observed in yeast [152]. Furthermore, our studies revealed a PGJ2-dependent decline in proteasome activity. This decline paralleled a shift of the 26S proteasome to the 20S core particle, indicating that PGJ2 disrupted the assembly state of 26S proteasomes. These findings support the notion that, like in yeast, the 20S proteasome is relatively inactive in SK-N-SH cells. Moreover, reduction in proteasome activity induced by J2 prostaglandins can reflect not only alterations in proteasome subunits but also disassembly of the 26S proteasome.

Besides altering the UPP, J2 prostaglandins also affect mitochondrial activity. Accordingly, 15d-PGJ2 induced a decrease in mitochondrial membrane potential in SH-SY5Y cells [42]. Furthermore, this form of J2 prostaglandin was recently shown to block oxygen consumption in intact mitochondria isolated from rat cerebral cortex [153]. This effect was mediated by inhibition of NADH dehydrogenase (ubiquinone) activity. Since this inhibition was abolished by DTT, it was suggested that 15d-PGJ2 forms a Michael adduct with a critical component of the mitochondrial complex 1 [153].

Taken together, these data suggest that mitochondrial dysfunction may be closely tied to 26S proteasome impairment. Assembly of the 26S proteasome into a functional complex capable of degrading ubiquitinated proteins is an ATP-dependent process. If impairment of mitochondrial function causes ATP-depletion, this would have a critical impact on 26S proteasome assembly leading to its inactivation and inability to degrade ubiquitinated proteins.

Overall, we conclude that products of inflammation, such as J2 prostaglandins, may play a crucial role in neurodegenerative disorders associated with the accumulation and aggregation of ubiquitinated proteins. A key question that remains unanswered is whether different forms of neurodegenerative disorders share a common mechanism, i.e. neuroinflammation. If so, how can the enormously varied etiology, presentation and time course of these devastating disorders be explained? For example, while head injury is a rapid, accidental event, PD is characterized by damage to specific brain regions resulting in motor disturbances and chronic degeneration [154]. This variety of disease manifestations could be correlated with the primary brain region affected by the injurious event, its severity and duration.

CHAPTER V

MODEL AND CONCLUSIONS

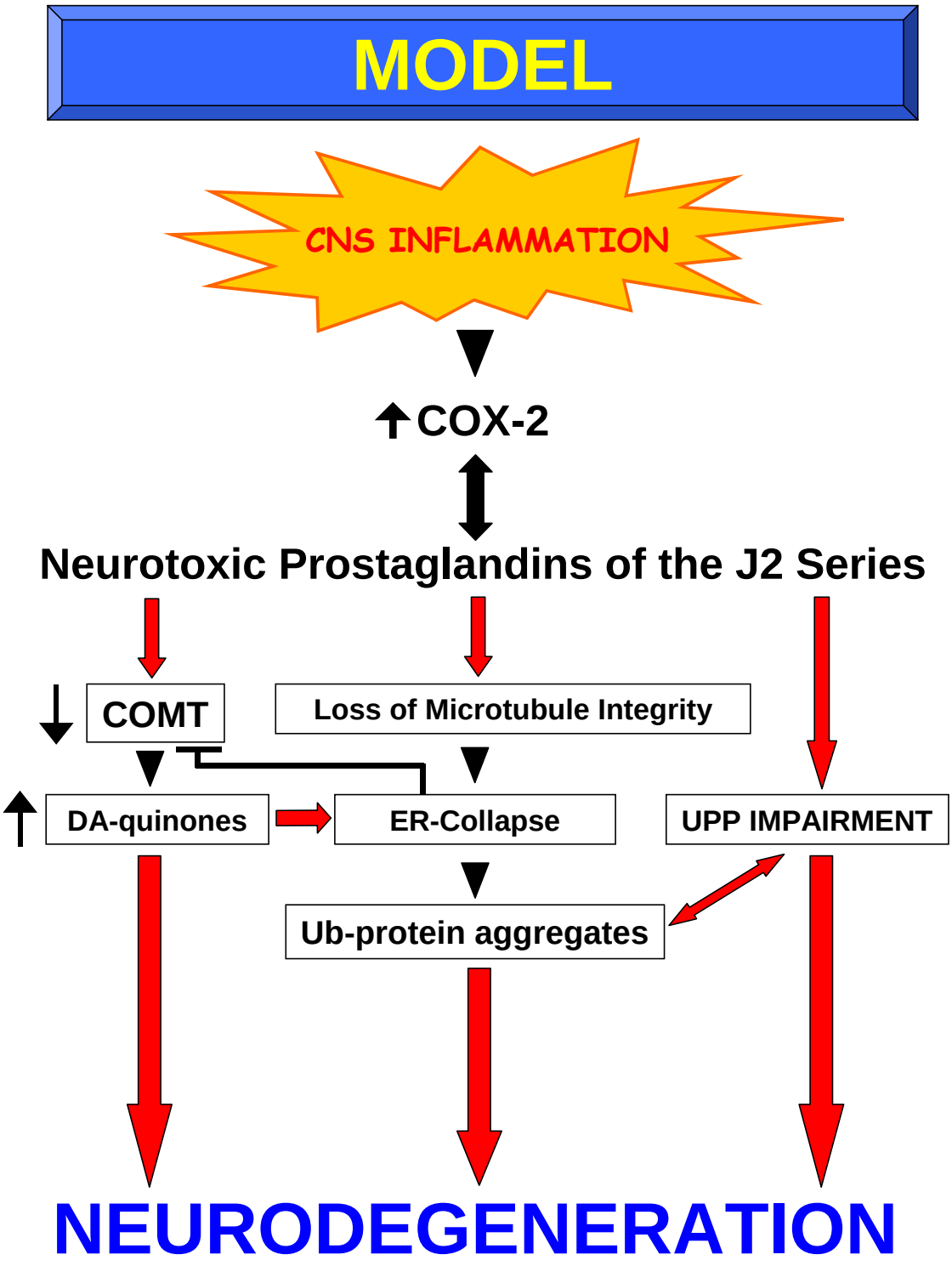
MODEL
CNS INFLAMMATION
COX-2
Neurotoxic Prostaglandins of the J2 Series
COMT
Loss of Microtubule Integrity
DA-quinones
ER-Collapse
UPP IMPAIRMENT
Ub-protein aggregates
NEURODEGENERATION

Our overall hypothesis is that infectious, chemical or physical insults in the CNS may initiate a cascade of events that leads to increased neuroinflammation leading to COX-2 up-regulation and prostaglandin production. Neurotoxic prostaglandins, such as PGJ2, perturb important cellular pathways involved in neuronal homeostasis. These prostanoids were shown to induce oxidative stress [42], disrupt the ubiquitin/proteasome pathway [44];[43], up-regulate COX-2 [33] and induce apoptosis [45].

We now demonstrate that PGJ2 impairs COMT activity, disrupts cytoskeleton integrity and impairs proteasome activity. If the damaging effects of PGJ2 cannot be reversed this will lead to protein aggregation. These protein aggregates may sequester "survival" proteins, such as heat shock proteins and metabolic enzymes including COMT. Once trapped in the aggregates these "survival" factors may no longer be able to reverse the damage induced by cellular stresses. Then pro-death pathways, including apoptosis, may be activated most likely to remove damaged cells. The resulting neuronal cell death may have devastating effects as, in the vast majority of cases, neurons lost to disease processes cannot be replaced. In conclusion, CNS inflammation is a potential risk factor to neurodegeneration.

CHAPTER VI

FUTURE DIRECTIONS

One major issue that remains to be solved is the ***in vivo*** concentrations of PGJ2 at sites affected in the various neurodegenerative disorders associated with inflammation. Notably, the levels of 15d-PGJ2, a PGJ2 metabolite, were shown to be elevated in spinal cord motor neurons of ALS patients [45]. In addition, J2 prostaglandins were detected in human body fluids [155] and human atherosclerotic plaques [91].

General physiological concentrations of prostaglandins in body fluids are found to be in the pico-nanomolar range, but their levels rise considerably under pathological conditions such as hyperthermia, infection and inflammation, reaching the micromolar range at the site of damage. Therefore, increases in the levels of PGJ2 produced by neurons and/or glia during inflammation associated with PD, AD and ALS neurodegeneration may critically exacerbate the neurodegenerative process.

Our data clearly show that PGJ2 is associated with the development of ubiquitinated protein aggregates. However, the direct or indirect nature of this association remains poorly defined. To address this question two experimental approaches are proposed.

6.1. Identify PGJ2 binding targets by affinity chromatography

The reactive α,β-unsaturated carbonyl group of J2 prostaglandins makes them susceptible to Michael addition reactions with free sulfhydryl groups on cellular proteins such as tubulin. This covalent biochemical reaction can occur endogenously thus perturbing the structure and/or activity of proteins with sulfhydryl groups.

Our data suggest that tubulin is a substrate for this reaction. However, showing a direct association between PGJ2 and tubulin would be important. One way to do this would be through affinity chromatography using biotinylated PGJ2. Once synthesized, biotinylated PGJ2 would be a valuable tool to apply in affinity chromatography methods with avidin/streptavidin beads, for identification of PGJ2-binding targets such as tubulin.

To date, there has been no demonstration of a direct association between PGJ2 and the 20S or 26S proteasomes. As such, affinity chromatography with biotinylated PGJ2 would also be an ideal experimental approach to investigate this putative association. This association may be independent of Michael addition.

Overall, the affinity chromatography strategy would be useful in identifying ***in vivo*** and ***in vitro*** associations of

PGJ2 with intracellular components relevant to neurodegeneration.

Our expectation would be that biotinylated PGJ2 would associate with 20S and 26S proteasomes. Previous studies have demonstrated cysteine-targeted protein oxidation by 15d-PGJ2. It is possible that PGJ2 may have a more direct interaction with cysteines on 20S and 26S proteasomes. Our approach would enable us to investigate this premise.

6.2. Investigate the correlation between PGJ2 neurotoxicity and the *in vivo* aggregation of ubiquitinated proteins

It is well-established that PGJ2 is neurotoxic and causes the accumulation of ubiquitinated protein aggregates. However, the time course of these two events has not been established. It is not clear to what extent protein aggregation affects cell viability or vice-versa.

This question could be addressed by the generation of a neuronal cell line stably transfected with a model UPP substrate consisting of a short degron fused to green fluorescent protein (GFP^{μ}), which renders GFP less stable. The time course of the accumulation of protein aggregates would be monitored by fluorescence microscopy. Cell death would be assessed by a live/dead assay for live cells

[LIVE/DEAD® Viability/Cytotoxicity Assay Kit; (Molecular Probes; Eugene, OR)].

To induce cell death and the accumulation of Ub-GFP^{u}, cells would be treated with PGJ2 or proteasome inhibitors, such as PSI. The time course of both events in an ***in vivo*** setting could then be compared. The data obtained would give an indication of the sequence in which these neurodegeneration associated events occur. Furthermore, if cells treated with PSI showed only increased Ub-GFP^{u} accumulation with little or no cell death, this would suggest that the accumulation of protein aggregates, per se, is not neurotoxic.

6.3. OVERALL CONCLUSION: In our view, it is critical to characterize the effects of neurotoxic products of inflammation. As we show in our studies, one of these products, PGJ2, recapitulates many of the pathological processes relevant to neurodegeneration. Abrogating the neurotoxicity of products of inflammation, such as PGJ2, is likely to be an effective therapeutic strategy to prevent and treat neurodegeneration.

CHAPTER VII

FIGURES

Figure 1 (next page) – PGJ2 alters *comt* gene expression – SK-N-SH cells were incubated at 37°C for 24h with the PGJ2 concentrations shown in the figure. Cells were harvested for semi-quantitative reverse transcription-PCR detection of *comt*, *seq.* and *gapdh* gene expression, as described in Materials and Methods. The PCR products for *comt* (817 bp), *seq.* (336 bp), *gapdh* (598 bp) and 18S rRNA (495 bp) are shown. The graphs represent the semi-quantification of the respective bands by densitometry. Data are shown as *comt*/18 rRNA (○) and *seq./gapdh* (●) ratios (represented by the number of pixels, arbitrary units) for each PGJ2 concentration as fold or percent change over control (vehicle only). Similar results were obtained in at least duplicate experiments. The size of the DNA fragments (in bp) is shown on the left.

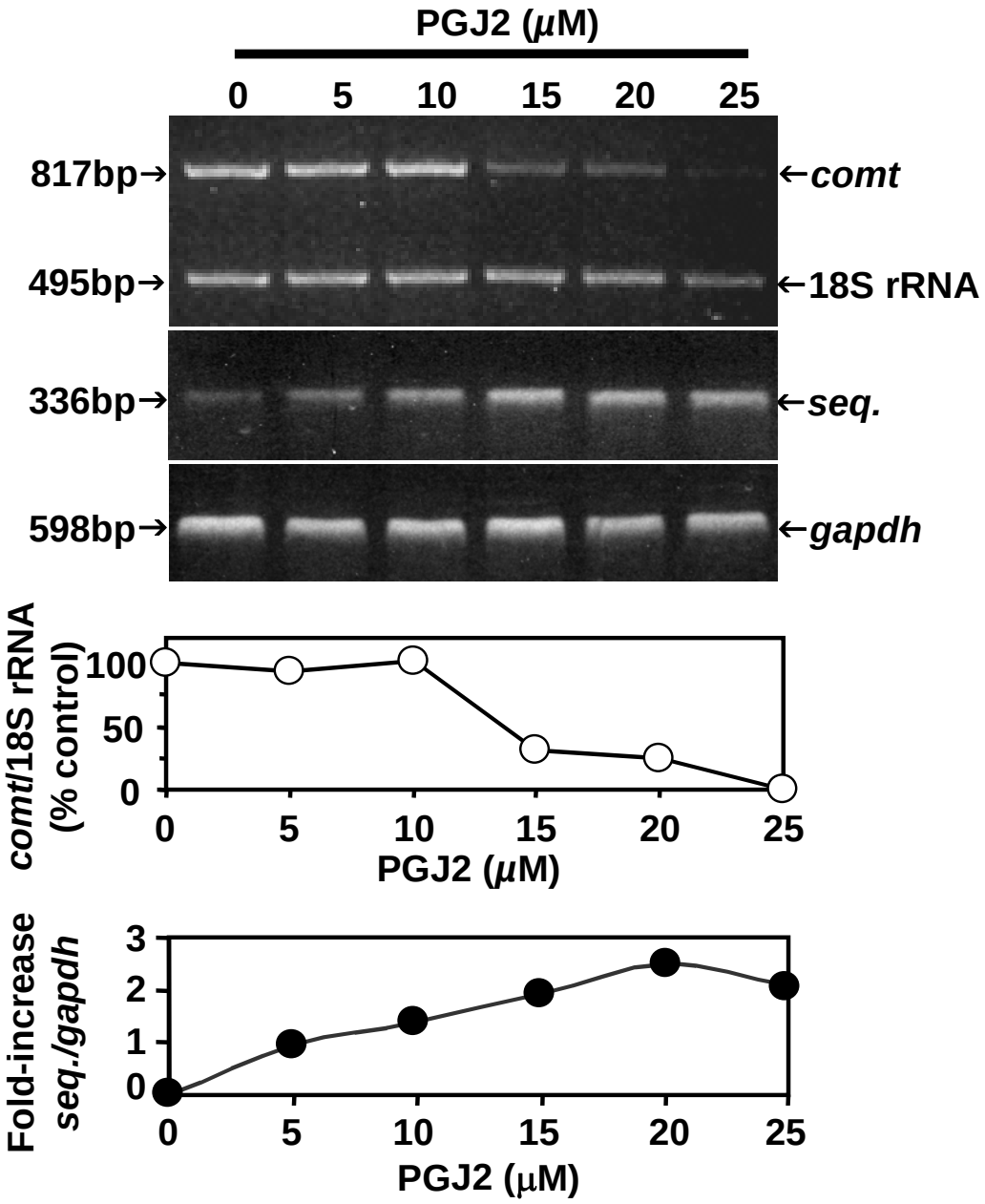
PGJ2 (μM)
0 5 10 15 20 25
817bp→
←comt
495bp→
←18S rRNA
336bp→
←seq.
598bp→
←gapdh
comt/18S rRNA (% control)
100
50
0
0 5 10 15 20 25
PGJ2 (μM)
Fold-increase seq./gapdh
3
2
1
0
0 5 10 15 20 25
PGJ2 (μM)

Figure 1

Figure 2 (next page) – PGJ2 alters COMT protein levels in a dose-dependent manner – Cells were harvested for Western blot analysis to detect MB-COMT (P2 fraction, 10 µg of protein/lane), S-COMT (S2 fraction, 20 µg of protein/lane) and Seq. (total lysate, 30 µg of protein/lane). Equal protein loading was demonstrated by probing the immunoblots for COX-1 (P2 fraction, middle panel, 10 µg of protein/lane and total lysate, bottom panel, 30 µg of protein/lane). The subcellular fractionation is described in Materials and Methods. The graphs represent the semi-quantification of the respective bands by densitometry. Data are shown as MB-COMT/COX-1 (□), S-COMT/COX-1 (■) and Seq./COX-1 (●) ratios (represented by the number of pixels, arbitrary units) for each PGJ2 concentration as fold or percent change over control (vehicle only). Similar results were obtained in at least duplicate experiments. The size of the protein bands (in kDa) is shown on the left.

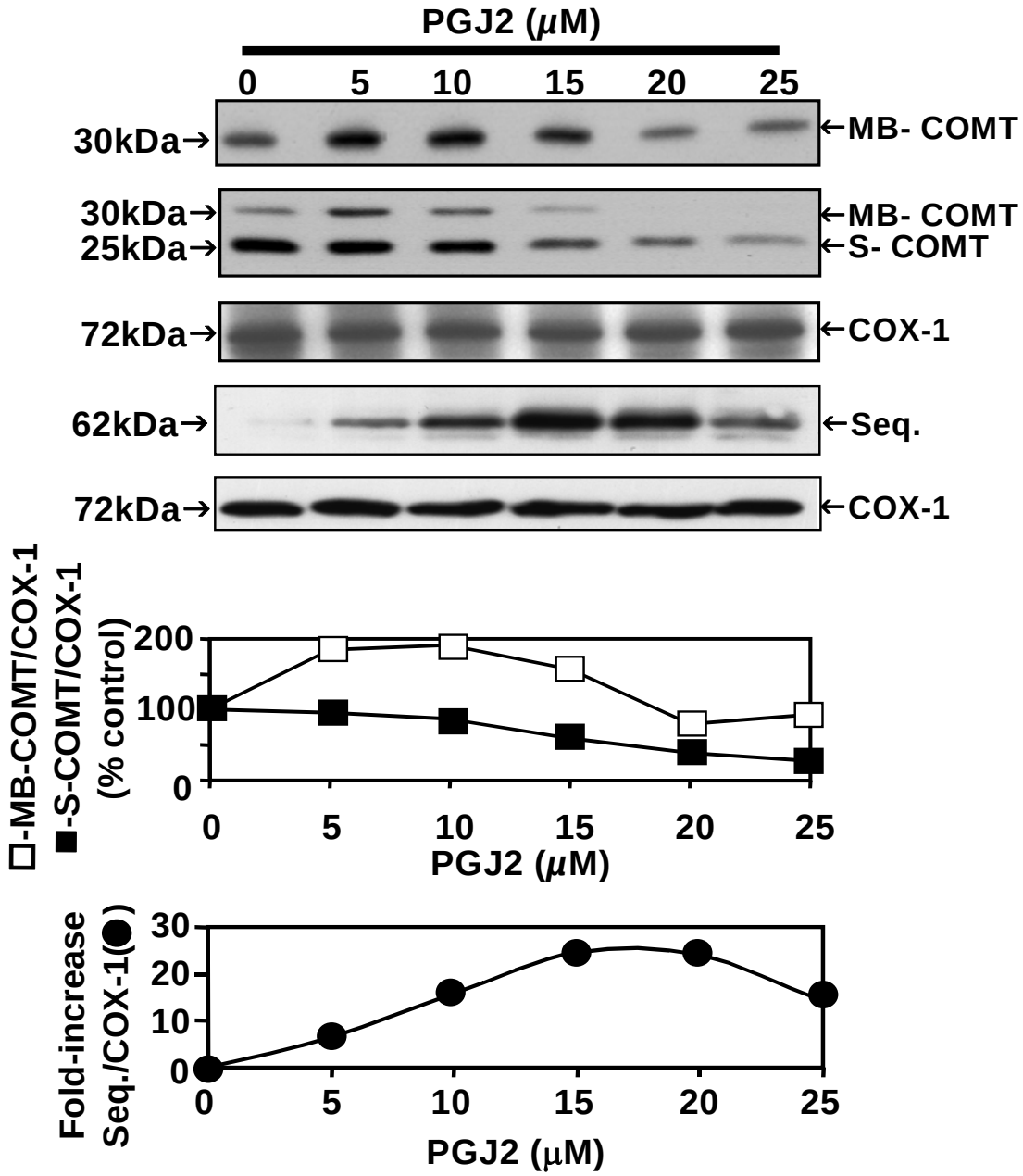
PGJ2 (μM)
0
5
10
15
20
25
30kDa→
←MB- COMT
30kDa→
25kDa→
←MB- COMT
←S- COMT
72kDa→
←COX-1
62kDa→
←Seq.
72kDa→
←COX-1
□-MB-COMT/COX-1
■-S-COMT/COX-1
(% control)
200
100
0
PGJ2 (μM)
Fold-increase
Seq./COX-1(●)
30
20
10
0
PGJ2 (μM)

Figure 2

Figure 3 – PGJ2 triggers the formation of large perinuclear aggregates containing COMT – Immunofluorescence staining of SK-N-SH cells treated with vehicle only (DMSO; ***A***, ***B***), 5 µM PGJ2 (***C***, ***D***) or 15 µM PGJ2 (***E***, ***F***) for 24 h. COMT was visualized by immunostaining with the anti-COMT antibody (***B***, ***D*** and ***F***, Texas Red). The nuclei (*n*) were detected with DAPI (***A***, ***C*** and ***E***); merged images are shown in (***A***, ***C*** and ***E***). The arrow is pointing to a large COMT aggregate.

Scale bar = 10 µm.

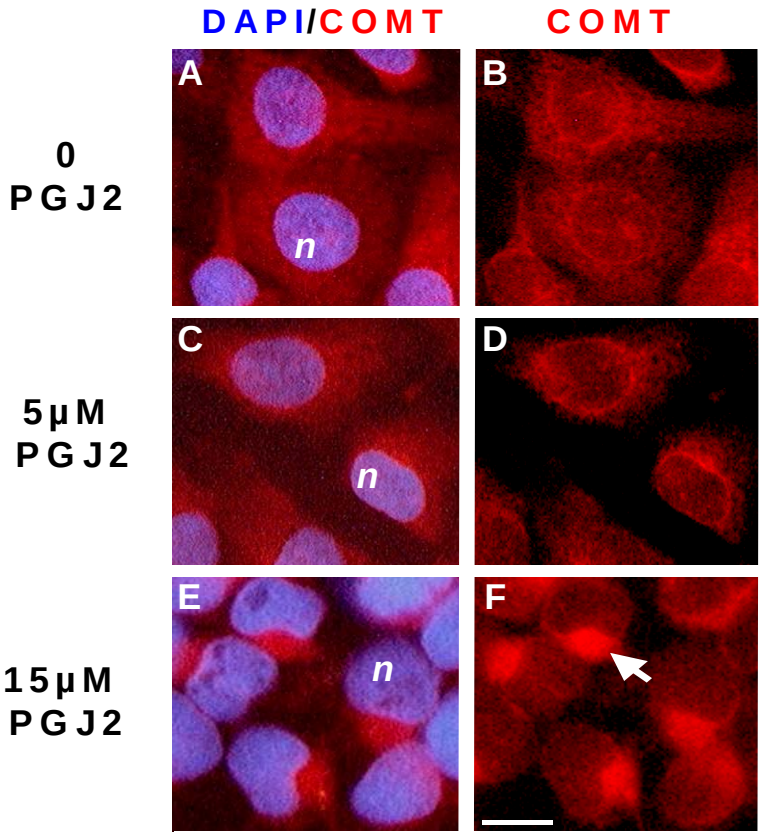

Figure 3

Figure 4 – PGJ2 induces the formation of aggresome-like structures in rat (P2) primary cortical neurons – Double immunofluorescence staining of rat (P2) cortical neurons treated with vehicle only (DMSO, ***A-C***) or 15 µM PGJ2 (***A'-C'***) for 24 h. The distribution of COMT was visualized with the anti-COMT antibody (***A and A'***, Texas Red) and the centrosome/MTOC with anti-γ-tubulin antibody (***B and B'***, FITC). Merged images are shown in (***C and C'***). The arrows are pointing to centrioles within the centrosome. Scale bar = 10 µm.

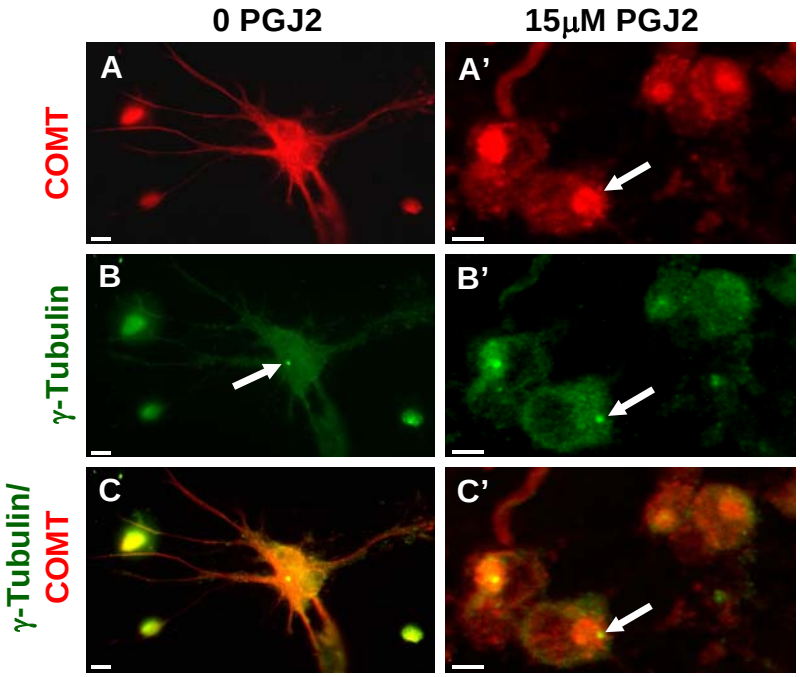

Figure 4

Figure 5 (next page) – PGJ2 alters the intracellular levels of *S*-adenosylmethionine (SAM) and dopamine metabolites – SK-N-SH cells were incubated at 37°C for 24 h with the PGJ2 and dopamine concentrations specified in the figure. Asterisks (*) identify the values that are significantly different ($P < 0.01$) from the control. **(A)** Intracellular SAM levels were measured as described in Materials and Methods. Data represent the mean ± SEM of four determinations. SAM levels for each condition were compared to those in cells treated with vehicle only (control, 100%). In the absence of PGJ2, SK-N-SH cells maintain a basal level of approximately 618.2 nmol of SAM/g of protein. **(B)** Intracellular dopamine (DA), 3,4-dihydroxy-phenyl-acetic acid (DOPAC), 3-methoxytyramine (3MT) and homovanillic acid (HVA) levels were measured as described in Materials and Methods. Data represent the mean (µmoles/g protein) from four determinations. (Insert) Dopamine catabolic pathways.

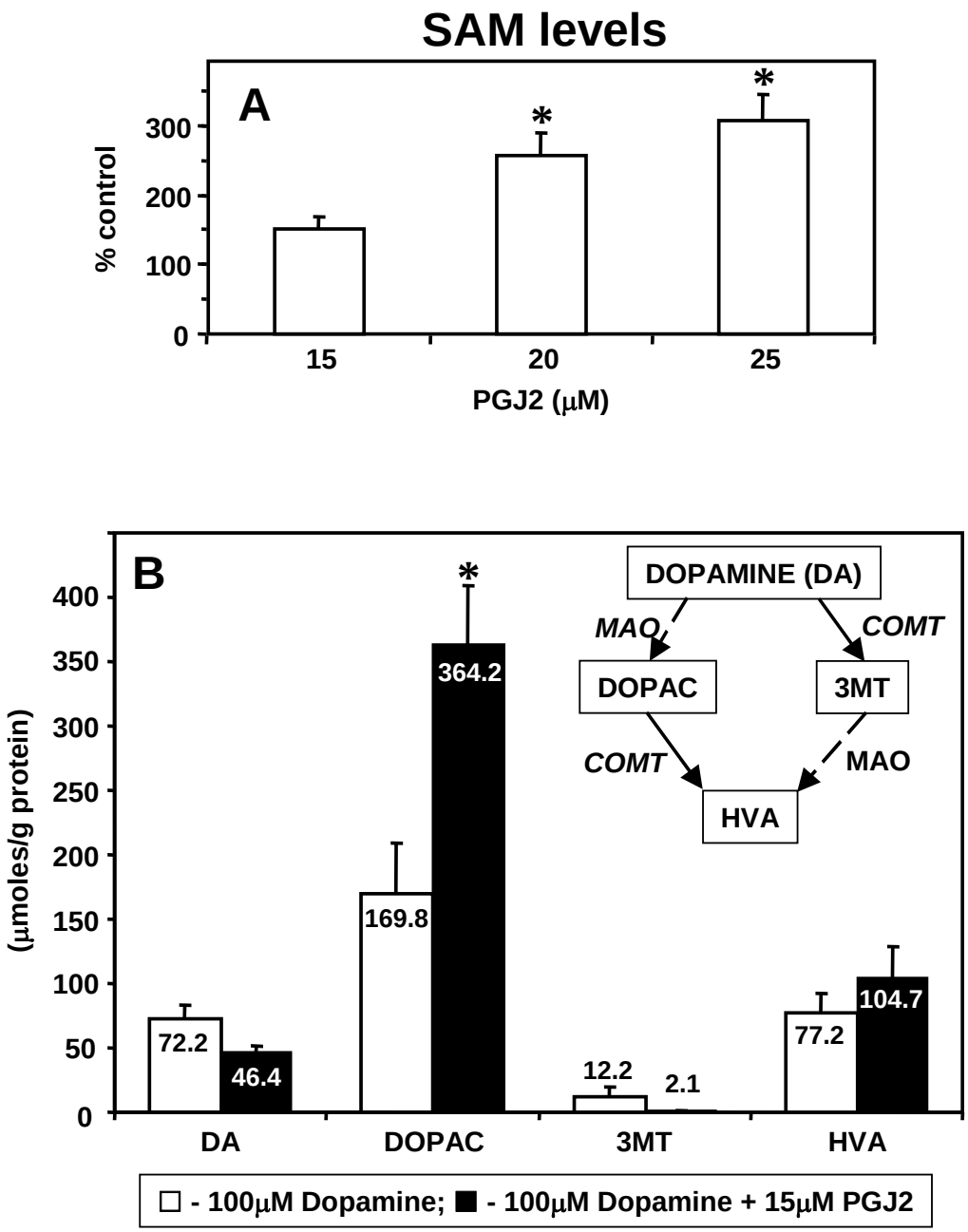
SAM levels
A
% control
0
100
200
300
*
*
15
20
25
PGJ2 (μM)
B
(μmoles/g protein)
0
50
100
150
200
250
300
350
400
*
364.2
169.8
72.2
46.4
12.2
2.1
77.2
104.7
DA
DOPAC
3MT
HVA
DOPAMINE (DA)
MAO
COMT
DOPAC
3MT
COMT
MAO
HVA
□ - 100μM Dopamine; ■ - 100μM Dopamine + 15μM PGJ2

Figure 5

Figure 6 – PGJ2 exacerbates dopamine toxicity – Viability of SK-N-SH cells treated with dopamine and vehicle only (DMSO, open circles), 5 μM PGJ2 (solid squares) or 15 μM PGJ2 (solid circles) for 24h. PGJ2 was added 6h prior to treatment with dopamine. Cell viability was assessed with the MTT assay (Materials and Methods). Data represent the mean ± SEM from at least three determinations. The viability for each condition was compared to the viability of cells treated with vehicle only (control, no PGJ2, no dopamine, 100%). Asterisks identify the values that are significantly different from the corresponding treatment with dopamine alone (*P < 0.01 and **P < 0.001).

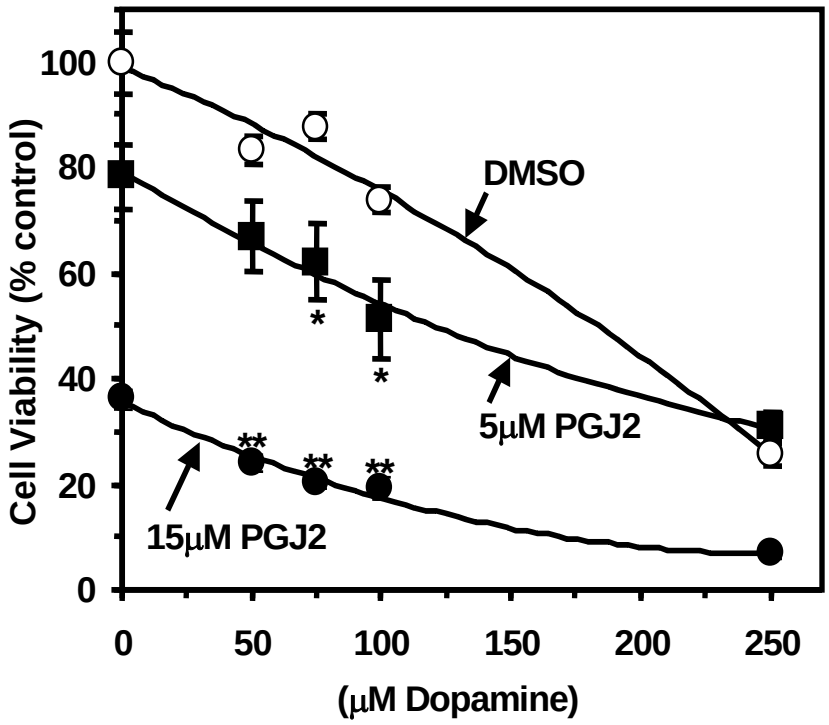

Figure 6

Figure 7 (next page) – PGJ2 perturbs the structure of the cytoskeleton – Immunofluorescence staining of SK-N-SH cells treated with vehicle only (DMSO, ***A, B*** and ***E***) or 15 µM PGJ2 (***C, D*** and ***F***) for 24h. Microtubules were visualized with an anti-α-tubulin antibody (***A, C, E*** and ***F***, Texas red) and actin filaments with an anti-actin antibody (***B*** and ***D***, FITC). (***n***) – nucleus. The scale bar = 10 µm.

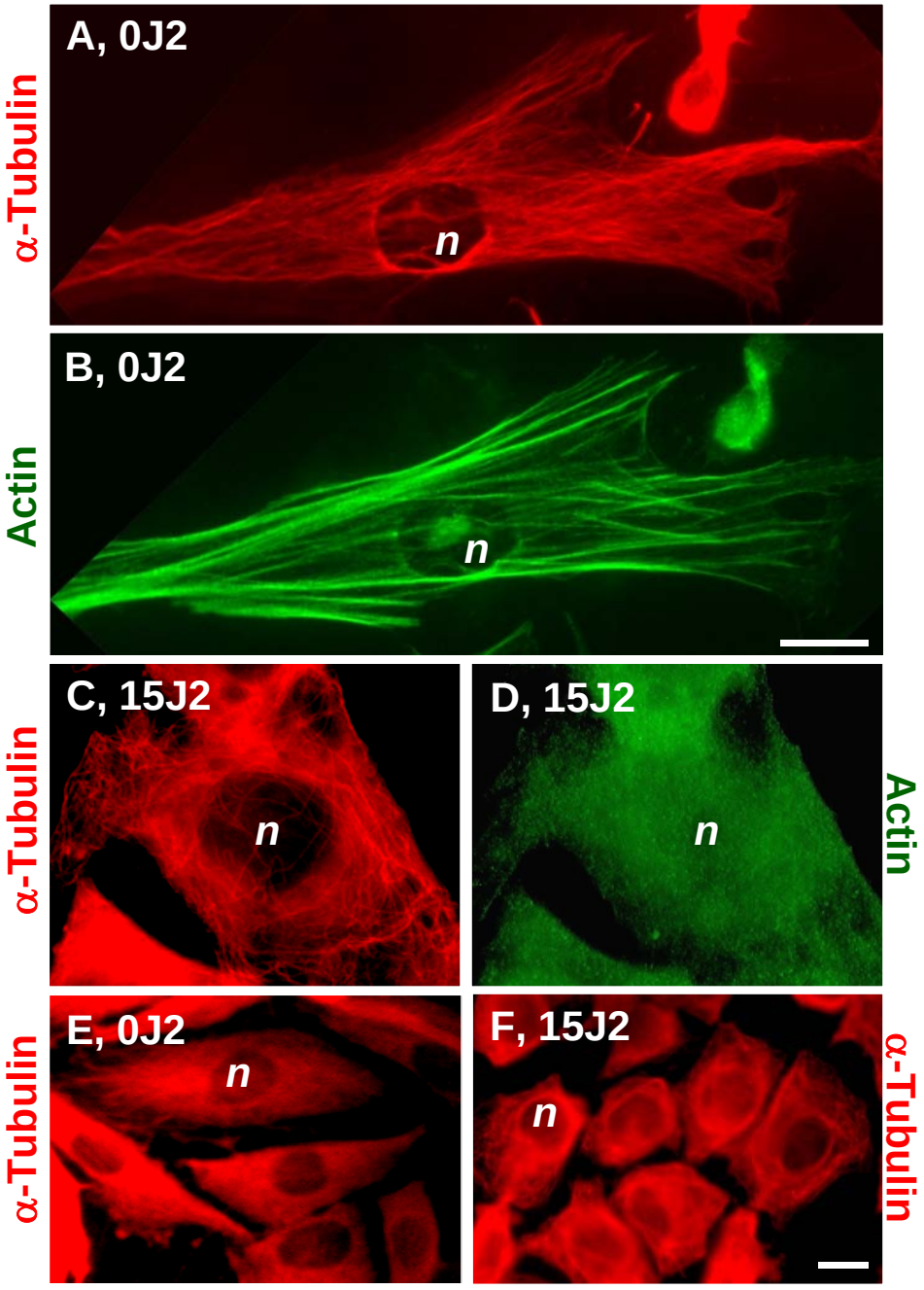
A, 0J2
α-Tubulin
n
B, 0J2
Actin
n
C, 15J2
α-Tubulin
n
D, 15J2
Actin
n
E, 0J2
α-Tubulin
n
F, 15J2
α-Tubulin
n

Figure 7

Figure 8 (next page) – PGJ2 hinders microtubule polymerization and decreases the number of tubulin free sulfhydryl groups – A – Tubulin polymerization was assayed in general tubulin buffer (GTB) with 1mM GTP and 2mM magnesium chloride in the absence of drugs (BLACK *open squares*) or in the presence of DMSO (1.5 %, BLUE *open squares*), or PGE2 (545 µM, BLUE *solid squares*), or PGJ2 (273 µM, RED *open squares*, 545 µM, RED *solid squares*) at 37°C in a 96-well plate. The increase in turbidity, indicative of tubulin polymerization, was monitored at 340 nm for ~30 min. The results represent the means of two independent determinations. **B** – The Vmax (mOD/min) for each reaction was determined with the KC4 Kineticalc program. **C** – Following incubation under the specified conditions, tubulin was denatured and its free sulfhydryls were assessed with DTNB. Absorbance was read at 405 nm. The results represent the means and SEM of three determinations.

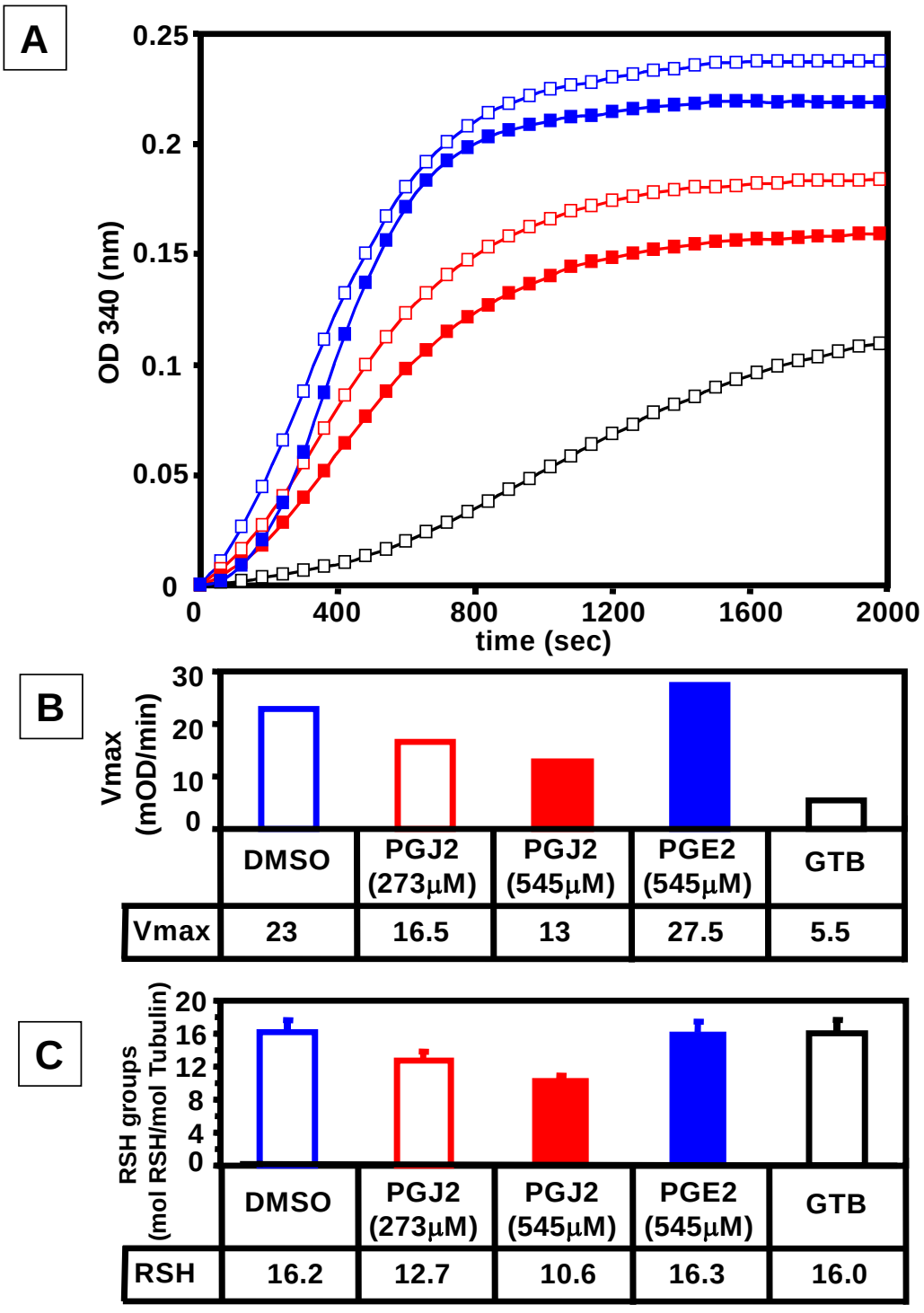
A
0.25
0.2
0.15
0.1
0.05
0
OD 340 (nm)
0
400
800
1200
1600
2000
time (sec)
B
Vmax (mOD/min)
30
20
10
0
DMSO
PGJ2 (273µM)
PGJ2 (545µM)
PGE2 (545µM)
GTB
Vmax
23
16.5
13
27.5
5.5
C
RSH groups (mol RSH/mol Tubulin)
20
16
12
8
4
0
DMSO
PGJ2 (273µM)
PGJ2 (545µM)
PGE2 (545µM)
GTB
RSH
16.2
12.7
10.6
16.3
16.0

Figure 8

Figure 9 (next page) – *In vitro* actin polymerization is not affected by PGJ2 - A – Actin polymerization was assessed in general actin buffer (GAB) with 0.2mM ATP and 0.2mM calcium chloride in the absence of drugs (*crosses*) or in the presence of DMSO (1.5 %, *open triangles*), or PGE2 (30 µM, *solid triangles*), or PGJ2 (30 µM, *open circles*, 545 µM, *solid circles*). Enhanced pyrene fluorescence, an indication of actin polymerization, was monitored at 365/407 nm for ~20 min. The results represent the means of two independent determinations. **B** – The Vmax (OD/min) for each reaction was determined with the KC4 Kineticalc program.

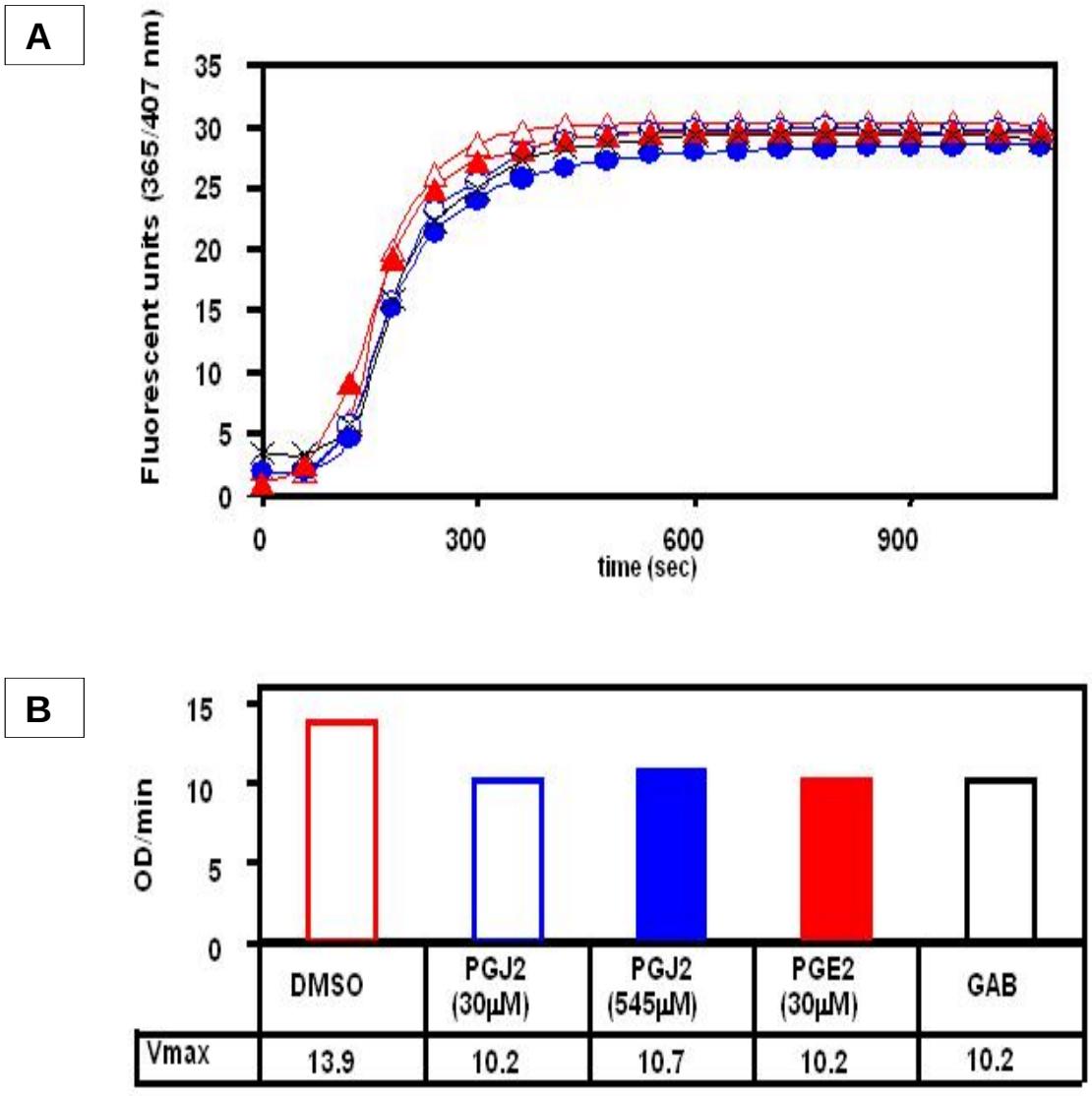
A
Fluorescent units (365/407 nm)
35
30
25
20
15
10
5
0
0
300
600
900
time (sec)
B
OD/min
15
10
5
0
DMSO
PGJ2 (30μM)
PGJ2 (545μM)
PGE2 (30μM)
GAB
Vmax
13.9
10.2
10.7
10.2
10.2

Figure 9

Figure 10 (next page) - PGJ2 triggers the collapse of the ER and formation of protein aggregates – Immunofluorescence staining of SK-N-SH cells treated with vehicle only (DMSO, ***A-C***), 5 µM PGJ2 (***D-F***) or 15 µM PGJ2 (***G-I***) for 24h. The ER was visualized by immunostaining for calnexin, an ER integral membrane protein (***B, E, H***, FITC) or with the anti-COMT antibody (***C, F, I,*** Texas Red). Nuclei (*n*) were detected with DAPI (***A***, ***D***, ***G***). *Arrows* point to large calnexin/COMT aggregates. The scale bar = 10 µm.

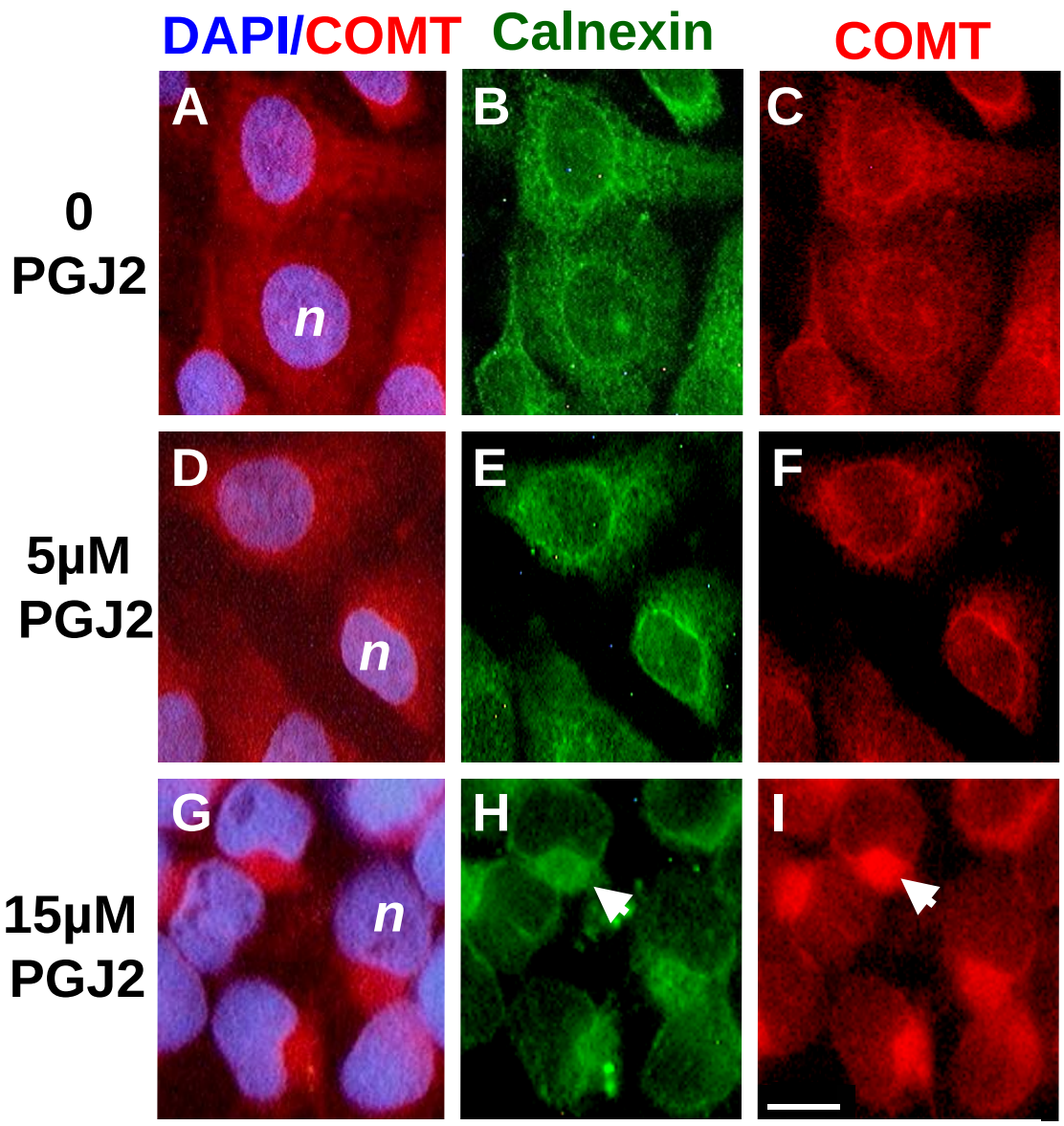
DAPI/COMT
Calnexin
COMT
0 PGJ2
5μM PGJ2
15μM PGJ2
A
B
C
D
E
F
G
H
I
n
n
n

Figure 10

Figure 11 – Disruption of the cytoskeleton by PGJ2 leads to development of aggregates co-localized with the centrosome – Double immunofluorescence staining of SK-N-SH cells treated with vehicle only (DMSO, ***A-D***) or 15 µM PGJ2 (***E-H***) for 24h. The distribution of COMT was visualized with the anti-COMT antibody (***C***, ***F***, Texas Red) and the centrosome/MTOC with the anti-γ-tubulin antibody (***D***, ***G***, FITC). Nuclei (*n*) were detected with DAPI (***A***, ***E***, blue). Merged images are shown in (***B***, ***H***). *Arrows* point to centrioles within the centrosome. The scale bar = 10 µm.

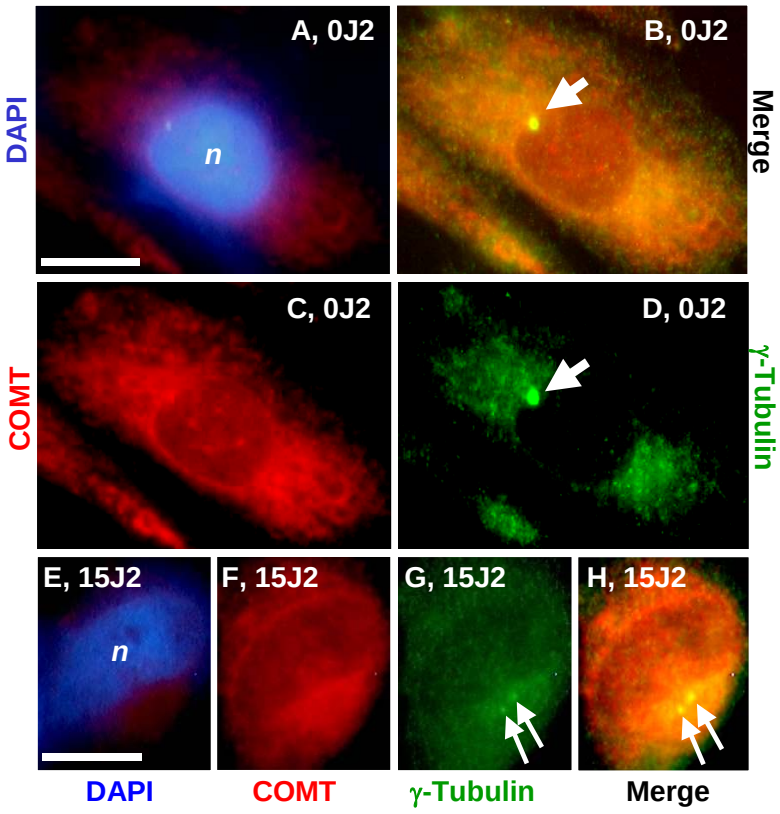

Figure 11

Figure 12 (next page) – Disruption of the cytoskeleton by PGJ2 coincides with formation of protein aggregates – Double immunofluorescence staining of SK-N-SH cells treated with 15 µM PGJ2 for 4h (***A, B***), 8h (***C, D***), 16h (***E, F***) and 24h (***G, H***). Microtubules were visualized with the anti-α-tubulin antibody (***A, C, E, G,*** Texas red), the centrosome/MTOC with the anti-γ-tubulin antibody (***B, D, F, H,*** FITC) and COMT with the anti-COMT antibody (***B, D, F, H,*** Texas Red). Merged images are shown in (***B, D, F, H***). The scale bar = 10 µm.

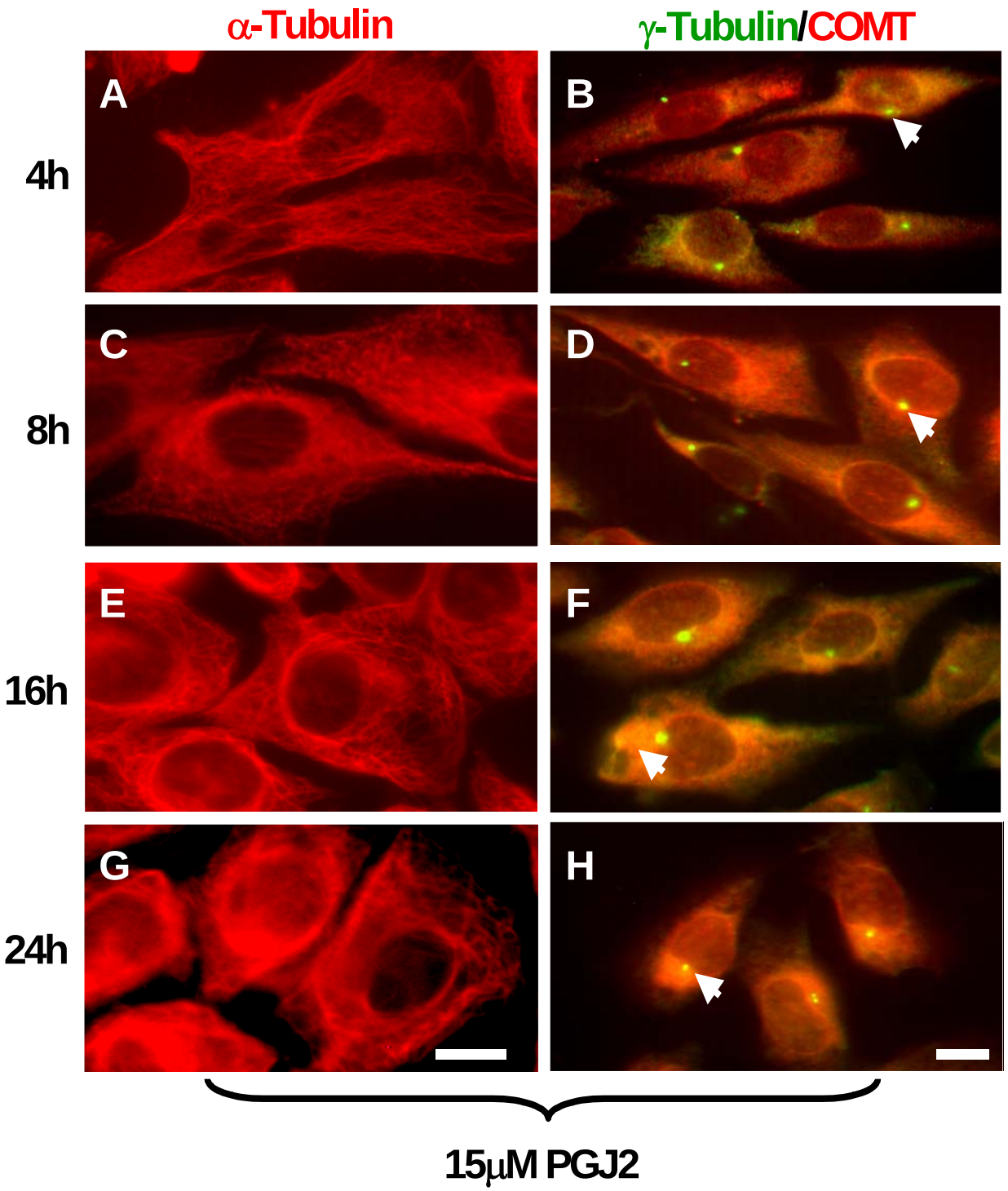

Figure 12

Figure 13 (next page) – Induction of protein aggregation following treatment with colchicine and brefeldin A – Double immunofluorescence staining of SK-N-SH cells treated for 24h with 15 µM colchicine (***A-C***), 15 µM brefeldin A (***D-H***) and vehicle (DMSO, ***I***). The distribution of ubiquitinated proteins was visualized with the anti-ubiquitinated proteins antibody (***A, D,*** Texas red), calnexin with the anti-calnexin antibody (***B, E,*** FITC) and microtubules with the anti-α-tubulin antibody (***C, H*** and ***I***, Texas red). Nuclei (*n*) were detected with DAPI (***G***, blue). Merged images are shown in (***F, G***). *Arrows* point to large perinuclear aggregates. The scale bar = 10 µm.

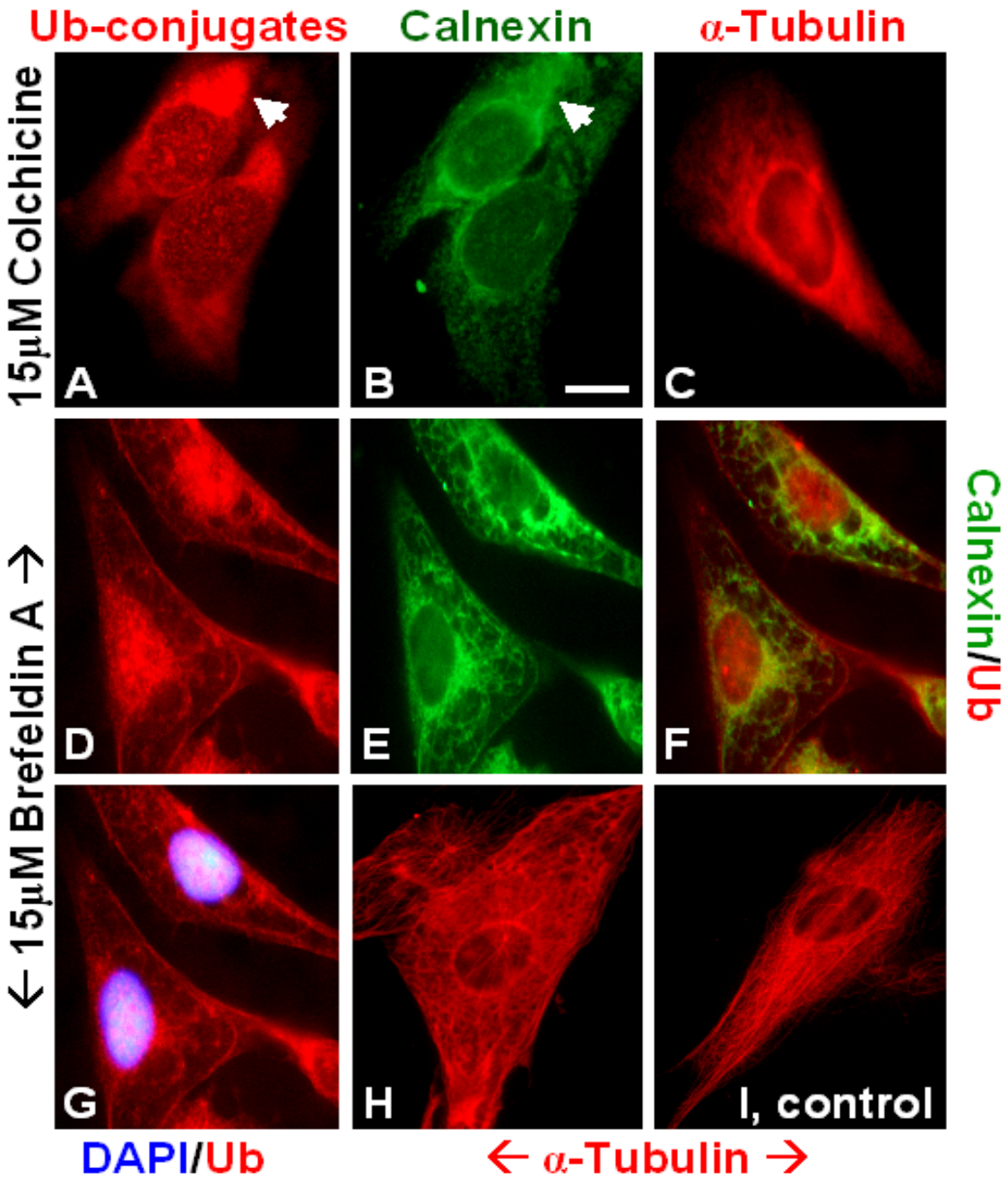
Ub-conjugates
Calnexin
α-Tubulin
15μM Colchicine
A
B
C
D
E
F
Calnexin/Ub
← 15μM Brefeldin A →
G
H
I, control
DAPI/Ub
← α-Tubulin →

Figure 13

Figure 14 (next page) - PGJ2 specifically induces the greatest accumulation of ubiquitinated proteins at 16h of treatment – Immunoblot of ubiquitinated proteins in SK-N-SH cells. Cells were harvested for Western blot analysis to detect ubiquitinated proteins (30 μg of protein/lane) after treatment with PGJ2 **(*Panel A*)**, brefeldin A **(*Panel B*)** and colchicine **(*Panel C*)** for 4, 8, 16 and 24h; and DMSO for 4 and 24h. Equal protein loading was demonstrated by reprobing the immunoblots for COX-1.

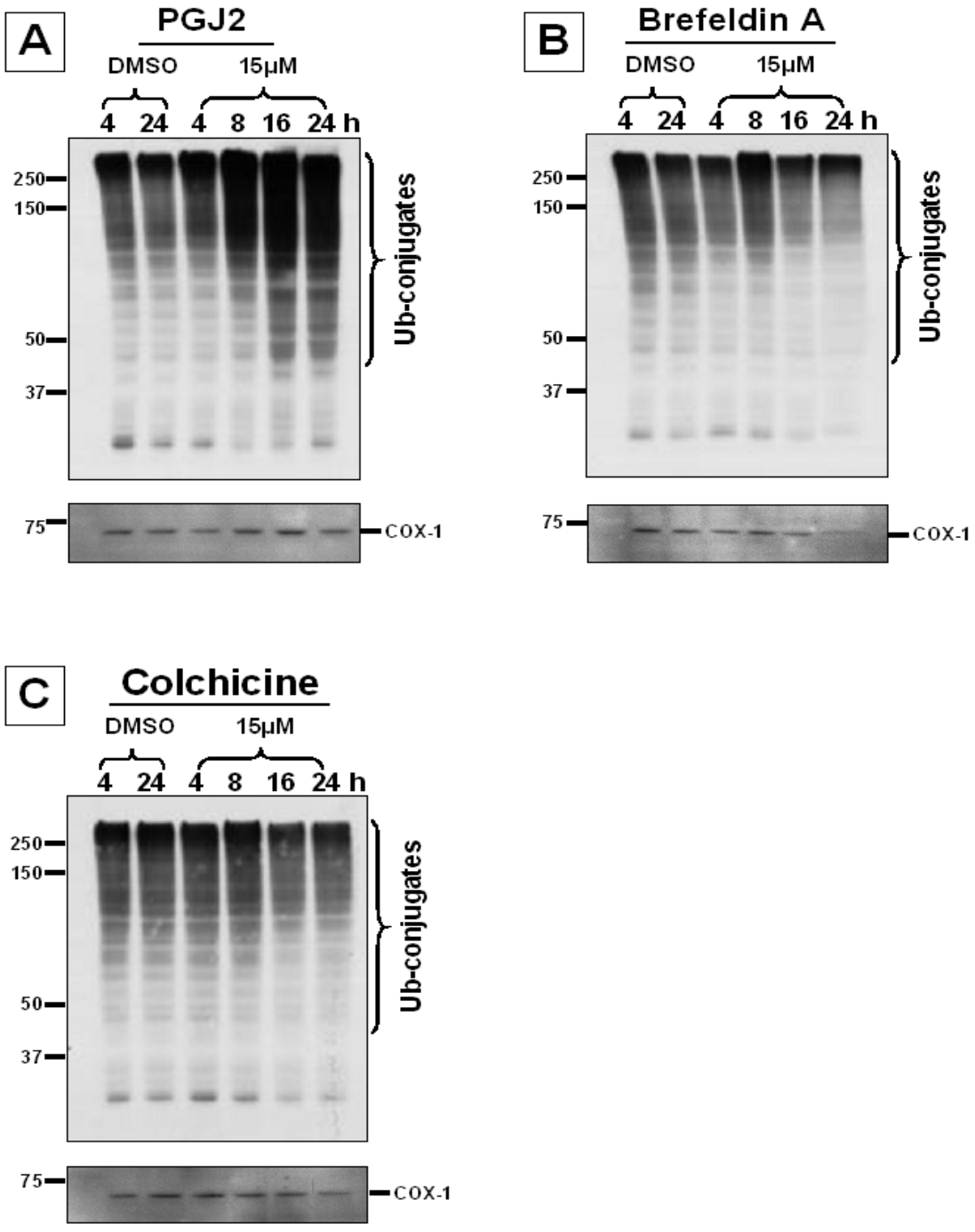
A
PGJ2
DMSO
15μM
4 24 4 8 16 24 h
250
150
50
37
Ub-conjugates
75
COX-1
B
Brefeldin A
DMSO
15μM
4 24 4 8 16 24 h
250
150
50
37
Ub-conjugates
75
COX-1
C
Colchicine
DMSO
15μM
4 24 4 8 16 24 h
250
150
50
37
Ub-conjugates
75
COX-1

Figure 14

Figure 15 (next page) – Detergent/salt-insoluble protein aggregates induced by PGJ2 contain ubiquitinated proteins Immunoblot of ubiquitinated proteins in SK-N-SH cells. Following a 24h treatment with DMSO (0, control) or 15 µM PGJ2 (15) total cell lysates (TL) were fractionated as described under (Materials and Methods). Equal protein amounts (5 µg) were loaded from each subcellular fraction listed. Similar results were obtained in duplicate experiments.

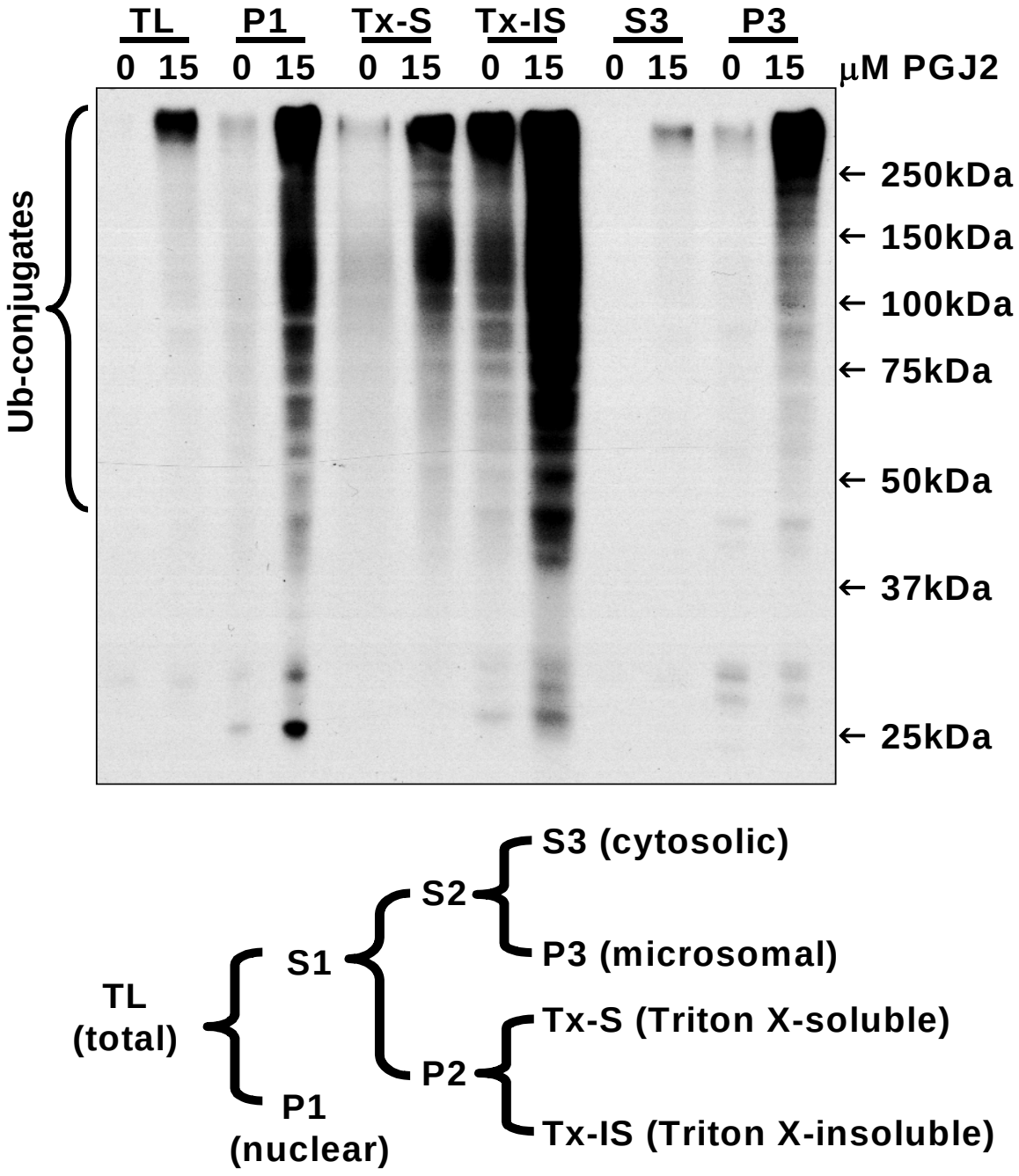
TL
P1
Tx-S
Tx-IS
S3
P3
0 15 0 15 0 15 0 15 0 15 0 15
μM PGJ2
Ub-conjugates
← 250kDa
← 150kDa
← 100kDa
← 75kDa
← 50kDa
← 37kDa
← 25kDa
S3 (cytosolic)
S2
P3 (microsomal)
S1
TL
(total)
Tx-S (Triton X-soluble)
P2
P1
(nuclear)
Tx-IS (Triton X-insoluble)

Figure 15

Figure 16 (next page) – Distribution of ubiquitinated proteins, α-synuclein and COMT in PGJ2-treated cells – Double immunofluorescence staining of SK-N-SH cells treated with vehicle only (DMSO, ***A-D*** and ***I-L***) or 15 µM PGJ2 (***E-H*** and ***M-P***) for 24h. The distribution of ubiquitinated proteins was visualized with anti-ubiquitinated proteins antibodies (***B, F,*** Texas red; ***J, N,*** FITC), α-synuclein with the anti-α-synuclein antibody (***C, G,*** FITC) and COMT with the anti-COMT antibody (***K, O,*** Texas Red). Nuclei (*n*) were detected with DAPI (***A, E, I, M,*** blue). Merged images are shown in (***D, H, L, P***). *Arrows* point to large perinuclear aggregates. The scale bar = 10 µm.

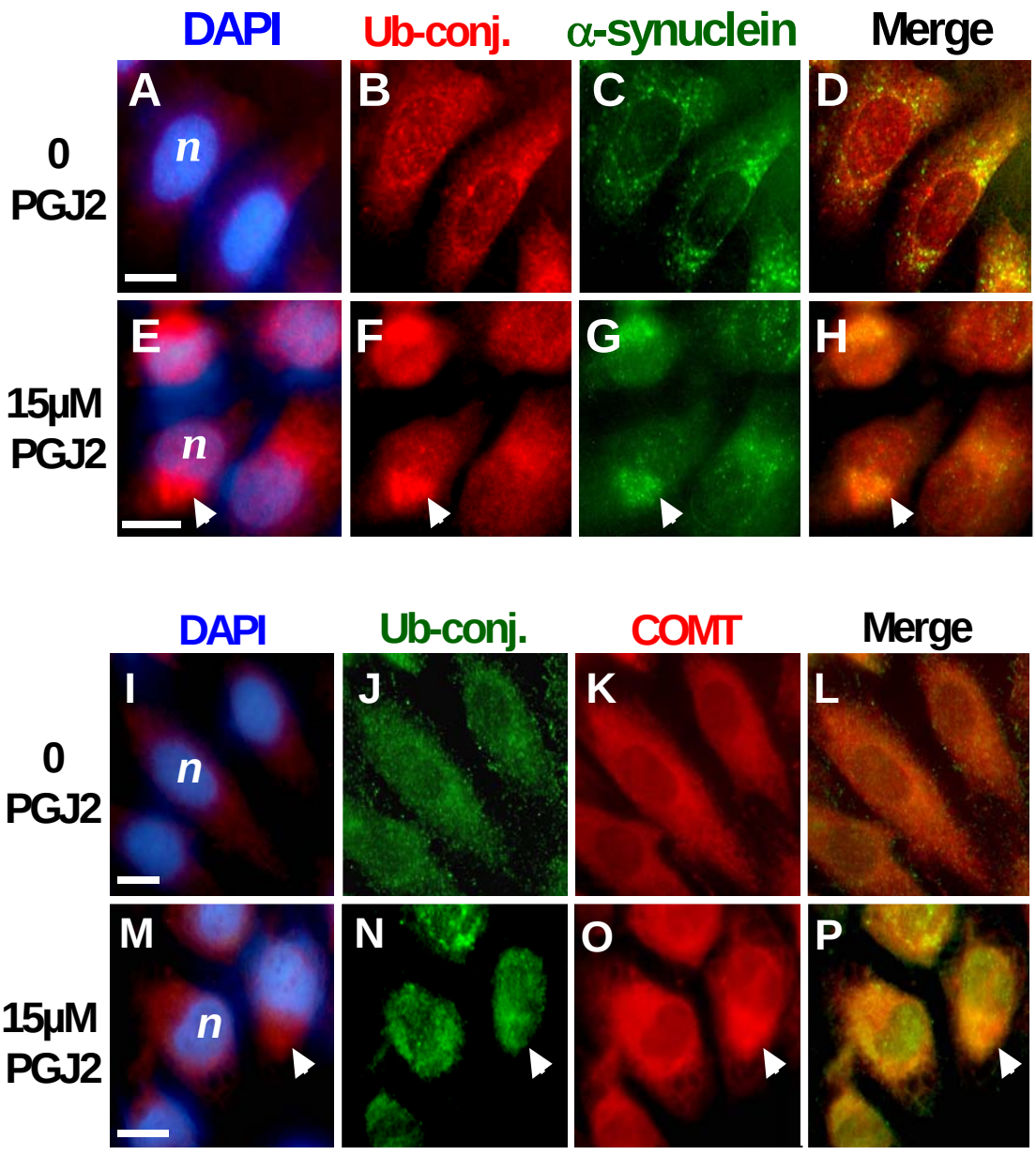
DAPI
Ub-conj.
α-synuclein
Merge
0 PGJ2
15μM PGJ2
A
B
C
D
E
F
G
H
n
DAPI
Ub-conj.
COMT
Merge
I
J
K
L
M
N
O
P

Figure 16

Figure 17 (next page) – Changes in proteasome assembly state in PGJ2-treated cells – Cleared lysates were prepared from SK-N-SH cells treated with DMSO (0.5 %, control) or 15 or 20 µM PGJ2 for 24h. Non-denaturing gel electrophoresis of the cell lysates, as well as of the 20S proteasome partially purified from rabbit reticulocyte lysates (marker), was performed as described under Materials and Methods. The chymotrypsin-like activity of the 26S proteasome holoenzyme, its core particle (20S proteasome) from SK-N-SH cells and the rabbit reticulocyte 20S proteasome were evaluated by an in-gel chymotrypsin-like activity (***left panel***). The relative abundance of the 26S, as well as the 20S proteasome in SK-N-SH cells treated under the different conditions, was assessed by immunoblotting with an antibody that reacts with the α4 subunit of the 20S proteasome (***middle panel***). The relative abundance of the 26S holoenzyme was assessed by stripping and reprobing the previous immunoblot with an antibody that reacts with the S8 (ATPase) subunit of the 19S regulatory particle (***right panel***). The 26S and the 20S forms of the proteasome are indicated on the left.

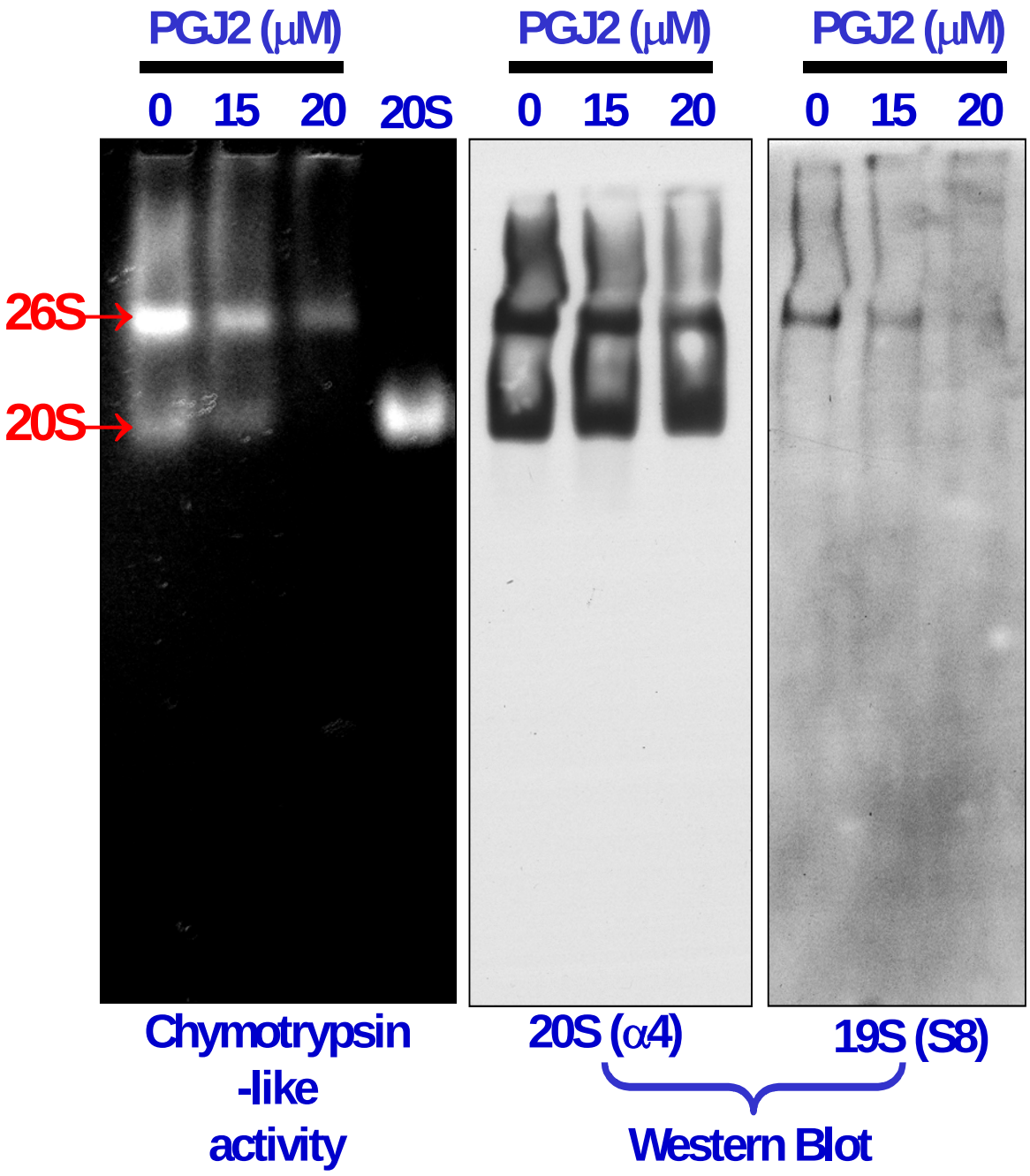
PGJ2 (μM)
PGJ2 (μM)
PGJ2 (μM)
0 15 20 20S
0 15 20
0 15 20
26S
20S
Chymotrypsin -like activity
20S (α4)
19S (S8)
Western Blot

Figure 17

CHAPTER VIII

REFERENCES

1. Gray DA, Tsirigotis M, Woulfe J. Ubiquitin, proteasomes, and the aging brain. ***Sci Aging Knowledge Environ*** 2003; 2003:RE6.

2. Lowe J, Blanchard A, Morrell K, Lennox G, Reynolds L, Billett M ***et al***. Ubiquitin is a common factor in intermediate filament inclusion bodies of diverse type in man, including those of Parkinson's disease, Pick's disease, and Alzheimer's disease, as well as Rosenthal fibres in cerebellar astrocytomas, cytoplasmic bodies in muscle, and mallory bodies in alcoholic liver disease. ***J Pathol*** 1988; 155:9-15.

3. Alves-Rodrigues A, Gregori L, Figueiredo-Pereira ME. Ubiquitin, cellular inclusions and their role in neurodegeneration. ***Trends Neurosci*** 1998; 21:516-520.

4. Wyss-Coray T, Mucke L. Inflammation in neurodegenerative disease--a double-edged sword. ***Neuron*** 2002; 35:419-432.

5. Li Z, Jansen M, Pierre S-R, Figueiredo-Pereira ME. Neurodegeneration: linking ubiquitin/proteasome pathway impairment with inflammation. ***Int J Biochem Cell Biol*** 2003; 35:547-552.

6. Consilvio C, Vincent AM, Feldman EL. Neuroinflammation, COX-2, and ALS--a dual role? ***Exp Neurol*** 2004; 187:1-10.

7. Markesbery WR, Carney JM. Oxidative alterations in Alzheimer's disease. ***Brain Pathol*** 1999; 9:133-146.

8. Fahn S, Cohen G. The oxidant stress hypothesis in Parkinson's disease: evidence supporting it. ***Ann Neurol*** 1992; 32:804-812.

9. Sadis S, Atienza CJ, Finley D. Synthetic signals for ubiquitin-dependent proteolysis. ***Mol Cell Biol*** 1995; 15:4086-4094.

10. Grune T, Reinheckel T, Davies KJ. Degradation of oxidized proteins in mammalian cells. ***FASEB J*** 1997; 11:526-534.

11. Chao CC, Ma YS, Stadtman ER. Modification of protein surface hydrophobicity and methionine oxidation by oxidative systems. ***Proc Natl Acad Sci U S A*** 1997; 94:2969-2974.

12. Dauer W, Przedborski S. Parkinson's disease: mechanisms and models. ***Neuron*** 2003; 39:889-909.

13. Flynn BL, Theesen KA. Pharmacologic management of Alzheimer disease part III: nonsteroidal antiinflammatory drugs--emerging protective evidence? ***Ann Pharmacother*** 1999; 33:840-849.

14. Stewart WF, Kawas C, Corrada M, Metter EJ. Risk of Alzheimer's disease and duration of NSAID use. ***Neurology*** 1997; 48:626-632.

15. Floyd RA. Antioxidants, oxidative stress, and degenerative neurological disorders. ***Proc Soc Exp Biol Med*** 1999; 222:236-245.

16. Dallner G, Sindelar PJ. Regulation of ubiquinone metabolism. ***Free Radic Biol Med*** 2000; 29:285-294.

17. Santa-Maria I, Smith MA, Perry G, Hernandez F, Avila J, Moreno FJ. Effect of quinones on microtubule polymerization: a link between oxidative stress and cytoskeletal alterations in Alzheimer's disease. ***Biochim Biophys Acta*** 2005; 1740:472-480.

18. Fukushima M. Prostaglandin J2--anti-tumour and anti-viral activities and the mechanisms involved. ***Eicosanoids*** 1990; 3:189-199.

19. Gilroy DW, Colville-Nash PR, Willis D, Chivers J, Paul-Clark MJ, Willoughby DA. Inducible cyclooxygenase may have anti-inflammatory properties. ***Nat Med*** 1999; 5:698-701.

20. Herschman HR, Reddy ST, Xie W. Function and regulation of prostaglandin synthase-2. ***Adv Exp Med Biol*** 1997; 407:61-66.

21. Smith WL. The eicosanoids and their biochemical mechanisms of action. ***Biochem J*** 1989; 259:315-324.

22. Scher JU, Pillinger MH. 15d-PGJ2: the anti-inflammatory prostaglandin? ***Clin Immunol*** 2005; 114:100-109.

23. Ide T, Egan K, Bell-Parikh LC, FitzGerald GA. Activation of nuclear receptors by prostaglandins. ***Thromb Res*** 2003; 110:311-315.

24. Kielian T, Drew PD. Effects of peroxisome proliferator-activated receptor-gamma agonists on central nervous system inflammation. ***J Neurosci Res*** 2003; 71:315-325.

25. Greene ME, Blumberg B, McBride OW, Yi HF, Kronquist K, Kwan K ***et al***. Isolation of the human peroxisome proliferator activated receptor gamma cDNA: expression in hematopoietic cells and chromosomal mapping. ***Gene Expr*** 1995; 4:281-299.

26. Braissant O, Foufelle F, Scotto C, Dauca M, Wahli W. Differential expression of peroxisome proliferator-activated receptors (PPARs): tissue distribution of PPAR-alpha, -beta, and -gamma in the adult rat. ***Endocrinology*** 1996; 137:354-366.

27. Azuma Y, Shinohara M, Wang PL, Ohura K. 15-Deoxy-delta(12,14)-prostaglandin J(2) inhibits IL-10 and IL-12 production by macrophages. ***Biochem Biophys Res Commun*** 2001; 283:344-346.

28. Nagy L, Tontonoz P, Alvarez JG, Chen H, Evans RM. Oxidized LDL regulates macrophage gene expression through ligand activation of PPARgamma. ***Cell*** 1998; 93:229-240.

29. Tontonoz P, Nagy L, Alvarez JG, Thomazy VA, Evans RM. PPARgamma promotes monocyte/macrophage differentiation and uptake of oxidized LDL. ***Cell*** 1998; 93:241-252.

30. Chinetti G, Fruchart JC, Staels B. Peroxisome proliferator-activated receptors (PPARs): nuclear receptors at the crossroads between lipid metabolism and inflammation. ***Inflamm Res*** 2000; 49:497-505.

31. Chinetti G, Gbaguidi FG, Griglio S, Mallat Z, Antonucci M, Poulain P ***et al***. CLA-1/SR-BI is expressed in atherosclerotic lesion macrophages and regulated by activators of peroxisome proliferator-activated receptors. ***Circulation*** 2000; 101:2411-2417.

32. Wilmer WA, Dixon C, Lu L, Hilbelink T, Rovin BH. A cyclopentenone prostaglandin activates mesangial MAP kinase independently of PPARgamma. ***Biochem Biophys Res Commun*** 2001; 281:57-62.

33. Li Z, Jansen M, Ogburn K, Salvatierra L, Hunter L, Mathew S ***et al***. Neurotoxic prostaglandin J2 enhances cyclooxygenase-2 expression in neuronal cells through the p38MAPK pathway: a death wish? ***J Neurosci Res*** 2004; 78:824-836.

34. Rossi A, Kapahi P, Natoli G, Takahashi T, Chen Y, Karin M ***et al***. Anti-inflammatory cyclopentenone prostaglandins are direct inhibitors of IkappaB kinase. ***Nature*** 2000; 403:103-108.

35. Straus DS, Pascual G, Li M, Welch JS, Ricote M, Hsiang CH ***et al***. 15-deoxy-delta 12,14-prostaglandin J2 inhibits multiple steps in the NF-kappa B signaling pathway. ***Proc Natl Acad Sci U S A*** 2000; 97:4844-4849.

36. Scher JU, Pillinger MH. 15d-PGJ2: the anti-inflammatory prostaglandin? ***Clin Immunol*** 2005; 114:100-109.

37. Straus DS, Glass CK. Cyclopentenone prostaglandins: new insights on biological activities and cellular targets. ***Med Res Rev*** 2001; 21:185-210.

38. Cernuda-Morollon E, Pineda-Molina E, Canada FJ, Perez-Sala D. 15-Deoxy-Delta 12,14-prostaglandin J2 inhibition of NF-kappaB-DNA binding through covalent modification of the p50 subunit. ***J Biol Chem*** 2001; 276:35530-35536.

39. Moos PJ, Edes K, Cassidy P, Massuda E, Fitzpatrick FA. Electrophilic prostaglandins and lipid aldehydes repress redox-sensitive transcription factors p53 and hypoxia-inducible factor by impairing the selenoprotein thioredoxin reductase. ***J Biol Chem*** 2003; 278:745-750.

40. Oliva JL, Perez-Sala D, Castrillo A, Martinez N, Canada FJ, Bosca L *et al.* The cyclopentenone 15-deoxy-delta 12,14-prostaglandin J2 binds to and activates H-Ras. ***Proc Natl Acad Sci U S A*** 2003; 100:4772-4777.

41. Kondo M, Shibata T, Kumagai T, Osawa T, Shibata N, Kobayashi M *et al.* 15-Deoxy-Delta(12,14)-prostaglandin J(2): the endogenous electrophile that induces neuronal apoptosis. ***Proc Natl Acad Sci U S A*** 2002; 99:7367-7372.

42. Kondo M, Oya-Ito T, Kumagai T, Osawa T, Uchida K. Cyclopentenone prostaglandins as potential inducers of intracellular oxidative stress. ***J Biol Chem*** 2001; 276:12076-12083.

43. Mullally JE, Moos PJ, Edes K, Fitzpatrick FA. Cyclopentenone prostaglandins of the J series inhibit the ubiquitin isopeptidase activity of the proteasome pathway. ***J Biol Chem*** 2001; 276:30366-30373.

44. Li Z, Melandri F, Berdo I, Jansen M, Hunter L, Wright S *et al.* delta12-Prostaglandin J2 inhibits the ubiquitin hydrolase UCH-L1 and elicits ubiquitin–protein aggregation without proteasome inhibition. ***Biochem Biophys Res Commun*** 2004; 319:1171-1180.

45. Kondo M, Shibata T, Kumagai T, Osawa T, Shibata N, Kobayashi M *et al.* 15-Deoxy-Delta(12,14)-prostaglandin J(2): the endogenous electrophile that induces neuronal apoptosis. ***Proc Natl Acad Sci U S A*** 2002; 99:7367-7372.

46. Harhangi BS, Farrer MJ, Lincoln S, Bonifati V, Meco G, De Michele G *et al.* The Ile93Met mutation in the ubiquitin carboxy-terminal-hydrolase-L1 gene is not observed in European cases with familial Parkinson's disease. ***Neurosci Lett*** 1999; 270:1-4.

47. Forno LS. Neuropathology of Parkinson's disease. ***J Neuropathol Exp Neurol*** 1996; 55:259-272.

48. Ghee M, Melki R, Michot N, Mallet J. PA700, the regulatory complex of the 26S proteasome, interferes with alpha-synuclein assembly. ***FEBS J*** 2005; 272:4023-4033.

49. Shang F, Gong X, Taylor A. Activity of ubiquitin-dependent pathway in response to oxidative stress. Ubiquitin-activating enzyme is transiently up-regulated. ***J Biol Chem*** 1997; 272:23086-23093.

50. Stokes AH, Hastings TG, Vrana KE. Cytotoxic and genotoxic potential of dopamine. ***J Neurosci Res*** 1999; 55:659-665.

51. Gao HM, Liu B, Hong JS. Critical role for microglial NADPH oxidase in rotenone-induced degeneration of dopaminergic neurons. ***J Neurosci*** 2003; 23:6181-6187.

52. Ren Y, Liu W, Jiang H, Jiang Q, Feng J. Selective vulnerability of dopaminergic neurons to microtubule depolymerization. ***J Biol Chem*** 2005; 280:34105-34112.

53. Stokes AH, Hastings TG, Vrana KE. Cytotoxic and genotoxic potential of dopamine. ***J Neurosci Res*** 1999; 55:659-665.

54. Mizuno Y, Ikebe S, Hattori N, Nakagawa-Hattori Y, Mochizuki H, Tanaka M ***et al***. Role of mitochondria in the etiology and pathogenesis of Parkinson's disease. ***Biochim Biophys Acta*** 1995; 1271:265-274.

55. Stadtman ER, Berlett BS. Reactive oxygen-mediated protein oxidation in aging and disease. ***Drug Metab Rev*** 1998; 30:225-243.

56. Grune T, Merker K, Sandig G, Davies KJ. Selective degradation of oxidatively modified protein substrates by the proteasome. ***Biochem Biophys Res Commun*** 2003; 305:709-718.

57. Dudek EJ, Shang F, Valverde P, Liu Q, Hobbs M, Taylor A. Selectivity of the ubiquitin pathway for oxidatively modified proteins: relevance to protein precipitation diseases. ***FASEB J*** 2005; 19:1707-1709.

58. Betarbet R, Sherer TB, Greenamyre JT. Ubiquitin-proteasome system and Parkinson's diseases. ***Exp Neurol*** 2005; 191 Suppl 1:S17-S27.

59. Sherman MY, Goldberg AL. Cellular defenses against unfolded proteins: a cell biologist thinks about neurodegenerative diseases. ***Neuron*** 2001; 29:15-32.

60. Cervera J, Levine RL. Modulation of the hydrophobicity of glutamine synthetase by mixed-function oxidation. ***FASEB J*** 1988; 2:2591-2595.

61. Davies KJ. Intracellular proteolytic systems may function as secondary antioxidant defenses: an hypothesis. ***J Free Radic Biol Med*** 1986; 2:155-173.

62. Davies KJ. Protein damage and degradation by oxygen radicals. I. general aspects. ***J Biol Chem*** 1987; 262:9895-9901.

63. Davies KJ. Degradation of oxidized proteins by the 20S proteasome. ***Biochimie*** 2001; 83:301-310.

64. Davies KJ, Delsignore ME. Protein damage and degradation by oxygen radicals. III. Modification of secondary and tertiary structure. ***J Biol Chem*** 1987; 262:9908-9913.

65. Davies KJ, Delsignore ME, Lin SW. Protein damage and degradation by oxygen radicals. II. Modification of amino acids. ***J Biol Chem*** 1987; 262:9902-9907.

66. Davies KJ, Lin SW, Pacifici RE. Protein damage and degradation by oxygen radicals. IV. Degradation of denatured protein. ***J Biol Chem*** 1987; 262:9914-9920.

67. Grune T, Davies KJ. The proteasomal system and HNE-modified proteins. ***Mol Aspects Med*** 2003; 24:195-204.

68. Reinheckel T, Sitte N, Ullrich O, Kuckelkorn U, Davies KJ, Grune T. Comparative resistance of the 20S and 26S proteasome to oxidative stress. ***Biochem J*** 1998; 335 (Pt 3):637-642.

69. Reinheckel T, Ullrich O, Sitte N, Grune T. Differential impairment of 20S and 26S proteasome activities in human hematopoietic K562 cells during oxidative stress. ***Arch Biochem Biophys*** 2000; 377:65-68.

70. Shringarpure R, Grune T, Mehlhase J, Davies KJ. Ubiquitin conjugation is not required for the degradation of oxidized proteins by proteasome. ***J Biol Chem*** 2003; 278:311-318.

71. Strack PR, Waxman L, Fagan JM. Activation of the multicatalytic endopeptidase by oxidants. Effects on enzyme structure. ***Biochemistry*** 1996; 35:7142-7149.

72. Reinheckel T, Sitte N, Ullrich O, Kuckelkorn U, Davies KJ, Grune T. Comparative resistance of the 20S and 26S proteasome to oxidative stress. ***Biochem J*** 1998; 335 (Pt 3):637-642.

73. Andersson M, Sjostrand J, Karlsson JO. Differential inhibition of three peptidase activities of the proteasome in human lens epithelium by heat and oxidation. ***Exp Eye Res*** 1999; 69:129-138.

74. Obin M, Shang F, Gong X, Handelman G, Blumberg J, Taylor A. Redox regulation of ubiquitin-conjugating enzymes: mechanistic insights using the thiol-specific oxidant diamide. ***FASEB J*** 1998; 12:561-569.

75. DeMartino GN. Purification of PA700, the 19S regulatory complex of the 26S proteasome. ***Methods Enzymol*** 2005; 398:295-306.

76. Ishii T, Sakurai T, Usami H, Uchida K. Oxidative modification of proteasome: identification of an oxidation-sensitive subunit in 26 s proteasome. ***Biochemistry*** 2005; 44:13893-13901.

77. Ogura T, Wilkinson AJ. AAA+ superfamily ATPases: common structure--diverse function. ***Genes Cells*** 2001; 6:575-597.

78. Choi HS, Seol W, Moore DD. A component of the 26S proteasome binds on orphan member of the nuclear hormone receptor superfamily. ***J Steroid Biochem Mol Biol*** 1996; 56:23-30.

79. Hartmann-Petersen R, Tanaka K, Hendil KB. Quaternary structure of the ATPase complex of human 26S proteasomes determined by chemical cross-linking. ***Arch Biochem Biophys*** 2001; 386:89-94.

80. Ohana B, Moore PA, Ruben SM, Southgate CD, Green MR, Rosen CA. The type 1 human immunodeficiency virus Tat binding protein is a transcriptional activator belonging to an additional family of evolutionarily conserved genes. ***Proc Natl Acad Sci U S A*** 1993; 90:138-142.

81. Uetz P, Giot L, Cagney G, Mansfield TA, Judson RS, Knight JR *et al*. A comprehensive analysis of protein-protein interactions in Saccharomyces cerevisiae. *Nature* 2000; 403:623-627.

82. Chao CC, Ma YS, Stadtman ER. Modification of protein surface hydrophobicity and methionine oxidation by oxidative systems. *Proc Natl Acad Sci U S A* 1997; 94:2969-2974.

83. Levine RL, Mosoni L, Berlett BS, Stadtman ER. Methionine residues as endogenous antioxidants in proteins. *Proc Natl Acad Sci U S A* 1996; 93:15036-15040.

84. Davies KJ, Shringarpure R. Preferential degradation of oxidized proteins by the 20S proteasome may be inhibited in aging and in inflammatory neuromuscular diseases. *Neurology* 2006; 66:S93-S96.

85. Guldberg HC, Marsden CA. Catechol-O-methyl transferase: pharmacological aspects and physiological role. *Pharmacol Rev* 1975; 27:135-206.

86. Mannisto PT, Kaakkola S. Catechol-O-methyltransferase (COMT): biochemistry, molecular biology, pharmacology, and clinical efficacy of the new selective COMT inhibitors. *Pharmacol Rev* 1999; 51:593-628.

87. Ogburn KD, Bottiglieri T, Wang Z, Figueiredo-Pereira ME. Prostaglandin J2 reduces catechol-O-methyltransferase activity and enhances dopamine toxicity in neuronal cells. *Neurobiol Dis* 2006.

88. McGeer PL, McGeer EG. Inflammation and the degenerative diseases of aging. *Ann N Y Acad Sci* 2004; 1035:104-116.

89. Yamagata K, Andreasson KI, Kaufmann WE, Barnes CA, Worley PF. Expression of a mitogen-inducible cyclooxygenase in brain neurons: regulation by synaptic activity and glucocorticoids. *Neuron* 1993; 11:371-386.

90. Consilvio C, Vincent AM, Feldman EL. Neuroinflammation, COX-2, and ALS--a dual role? *Exp Neurol* 2004; 187:1-10.

91. Shibata T, Kondo M, Osawa T, Shibata N, Kobayashi M, Uchida K. 15-deoxy-delta 12,14-prostaglandin J2. A prostaglandin D2 metabolite generated during inflammatory processes. ***J Biol Chem*** 2002; 277:10459-10466.

92. Fukushima M. Prostaglandin J2--anti-tumour and anti-viral activities and the mechanisms involved. ***Eicosanoids*** 1990; 3:189-199.

93. Herschman HR, Reddy ST, Xie W. Function and regulation of prostaglandin synthase-2. ***Adv Exp Med Biol*** 1997; 407:61-66.

94. Gilroy DW, Colville-Nash PR, Willis D, Chivers J, Paul-Clark MJ, Willoughby DA. Inducible cyclooxygenase may have anti-inflammatory properties [see comments]. ***Nat Med*** 1999; 5:698-701.

95. Mannisto PT, Kaakkola S. Catechol-O-methyltransferase (COMT): biochemistry, molecular biology, pharmacology, and clinical efficacy of the new selective COMT inhibitors. ***Pharmacol Rev*** 1999; 51:593-628.

96. McGeer EG, Kremer B, Hayden MR. Monoamines and their metabolites in Huntington's disease brain: evidence for decreased catechol-O-methyltransferase activity. ***Biol Psychiatry*** 1993; 33:551-553.

97. Tai CH, Wu RM. Catechol-O-methyltransferase and Parkinson's disease. ***Acta Med Okayama*** 2002; 56:1-6.

98. Hong J, Shu-Leong H, Tao X, Lap-Ping Y. Distribution of catechol-O-methyltransferase expression in human central nervous system. ***Neuroreport*** 1998; 9:2861-2864.

99. Rivett AJ, Francis A, Roth JA. Distinct cellular localization of membrane-bound and soluble forms of catechol-O-methyltransferase in brain. ***J Neurochem*** 1983; 40:215-219.

100. Petrucelli L, Dickson D, Kehoe K, Taylor J, Snyder H, Grover A ***et al***. CHIP and Hsp70 regulate tau ubiquitination, degradation and aggregation. ***Hum Mol Genet*** 2004; 13:703-714.

101. Biedler JL, Roffler-Tarlov S, Schachner M, Freedman LS. Multiple neurotransmitter synthesis by human neuroblastoma cell lines and clones. ***Cancer Res*** 1978; 38:3751-3757.

102. Siddiq MM, Tsirka SE. Modulation of zinc toxicity by tissue plasminogen activator. ***Mol Cell Neurosci*** 2004; 25:162-171.

103. Matsumoto M, Weickert CS, Akil M, Lipska BK, Hyde TM, Herman MM ***et al***. Catechol O-methyltransferase mRNA expression in human and rat brain: evidence for a role in cortical neuronal function. ***Neuroscience*** 2003; 116:127-137.

104. Bottiglieri T. Isocratic high performance liquid chromatographic analysis of S-adenosylmethionine and S-adenosylhomocysteine in animal tissues: the effect of exposure to nitrous oxide. ***Biomed Chromatogr*** 1990; 4:239-241.

105. Mosmann T. Rapid colorimetric assay for cellular growth and survival: application to proliferation and cytotoxicity assays. ***J Immunol Methods*** 1983; 65:55-63.

106. Wang Z, Figueiredo-Pereira ME. Inhibition of sequestosome 1/p62 up-regulation prevents aggregation of ubiquitinated proteins induced by prostaglandin J2 without reducing its neurotoxicity. ***Mol Cell Neurosci*** 2005; 29:222-231.

107. Smith WL, DeWitt DL, Garavito RM. Cyclooxygenases: structural, cellular, and molecular biology. ***Annu Rev Biochem*** 2000; 69:145-182.

108. Rosenberg PA. Catecholamine toxicity in cerebral cortex in dissociated cell culture. ***J Neurosci*** 1988; 8:2887-2894.

109. Lode HN, Bruchelt G, Seitz G, Gebhardt S, Gekeler V, Niethammer D ***et al***. Reverse transcriptase-polymerase chain reaction (RT-PCR) analysis of monoamine transporters in neuroblastoma cell lines: correlations to meta-iodobenzylguanidine (MIBG) uptake and tyrosine hydroxylase gene expression. ***Eur J Cancer*** 1995; 31A:586-590.

110. Zhu BT. Catechol-O-Methyltransferase (COMT)-mediated methylation metabolism of endogenous bioactive catechols and modulation by endobiotics and xenobiotics: importance in pathophysiology and pathogenesis. ***Curr Drug Metab*** 2002; 3:321-349.

111. Xie T, Ho SL, Ramsden D. Characterization and implications of estrogenic down-regulation of human catechol-O-methyltransferase gene transcription. ***Mol Pharmacol*** 1999; 56:31-38.

112. Takahashi S, Odani N, Tomokiyo K, Furuta K, Suzuki M, Ichikawa A ***et al***. Localization of a cyclopentenone prostaglandin to the endoplasmic reticulum and induction of BiP mRNA. ***Biochem J*** 1998; 335 (Pt 1):35-42.

113. Saito S, Takahashi S, Takagaki N, Hirose T, Sakai T. 15-Deoxy-Delta(12,14)-prostaglandin J2 induces apoptosis through activation of the CHOP gene in HeLa cells. ***Biochem Biophys Res Commun*** 2003; 311:17-23.

114. Ulmanen I, Peranen J, Tenhunen J, Tilgmann C, Karhunen T, Panula P ***et al***. Expression and intracellular localization of catechol O-methyltransferase in transfected mammalian cells. ***Eur J Biochem*** 1997; 243:452-459.

115. Greenamyre JT, Hastings TG. Biomedicine. Parkinson's--divergent causes, convergent mechanisms. ***Science*** 2004; 304:1120-1122.

116. Kastner A, Anglade P, Bounaix C, Damier P, Javoy-Agid F, Bromet N ***et al***. Immunohistochemical study of catechol-O-methyltransferase in the human mesostriatal system. ***Neuroscience*** 1994; 62:449-457.

117. Zhu BT. CNS dopamine oxidation and catechol-O-methyltransferase: importance in the etiology, pharmacotherapy, and dietary prevention of Parkinson's disease. ***Int J Mol Med*** 2004; 13:343-353.

118. Cohen G. Oxidative stress, mitochondrial respiration, and Parkinson's disease. ***Ann N Y Acad Sci*** 2000; 899:112-120.

119. Werner P, Di Rocco A, Prikhojan A, Rempel N, Bottiglieri T, Bressman S *et al.* COMT-dependent protection of dopaminergic neurons by methionine, dimethionine and S-adenosylmethionine (SAM) against L-dopa toxicity in vitro. ***Brain Res*** 2001; 893:278-281.

120. Ross CA, Poirier MA. Opinion: What is the role of protein aggregation in neurodegeneration? ***Nat Rev Mol Cell Biol*** 2005; 6:891-898.

121. Pignatelli M, Sanchez-Rodriguez J, Santos A, Perez-Castillo A. 15-Deoxy-{Delta}-12,14-prostaglandin J2 induces programmed cell death of breast cancer cells by a pleiotropic mechanism. ***Carcinogenesis*** 2005; 26:81-92.

122. Landino LM, Hasan R, McGaw A, Cooley S, Smith AW, Masselam K *et al.* Peroxynitrite oxidation of tubulin sulfhydryls inhibits microtubule polymerization. ***Arch Biochem Biophys*** 2002; 398:213-220.

123. Liu CL, Ge P, Zhang F, Hu BR. Co-translational protein aggregation after transient cerebral ischemia. ***Neuroscience*** 2005; 134:1273-1284.

124. Himes RH, Burton PR, Gaito JM. Dimethyl sulfoxide-induced self-assembly of tubulin lacking associated proteins. ***J Biol Chem*** 1977; 252:6222-6228.

125. Ishii T, Uchida K. Induction of reversible cysteine-targeted protein oxidation by an endogenous electrophile 15-deoxy-delta12,14-prostaglandin J2. ***Chem Res Toxicol*** 2004; 17:1313-1322.

126. Ponstingl H, Krauhs E, Little M, Kempf T. Complete amino acid sequence of alpha-tubulin from porcine brain. ***Proc Natl Acad Sci U S A*** 1981; 78:2757-2761.

127. Krauhs E, Little M, Kempf T, Hofer-Warbinek R, Ade W, Ponstingl H. Complete amino acid sequence of beta-tubulin from porcine brain. ***Proc Natl Acad Sci U S A*** 1981; 78:4156-4160.

128. Terasaki M, Chen LB, Fujiwara K. Microtubules and the endoplasmic reticulum are highly interdependent structures. ***J Cell Biol*** 1986; 103:1557-1568.

129. Baumann O, Walz B. Endoplasmic reticulum of animal cells and its organization into structural and functional domains. ***Int Rev Cytol*** 2001; 205:149-214.

130. Johnston JA, Ward CL, Kopito RR. Aggresomes: a cellular response to misfolded proteins. ***J Cell Biol*** 1998; 143:1883-1898.

131. Kopito RR. Aggresomes, inclusion bodies and protein aggregation. ***Trends Cell Biol*** 2000; 10:524-530.

132. Masliah E, Rockenstein E, Adame A, Alford M, Crews L, Hashimoto M ***et al***. Effects of alpha-synuclein immunization in a mouse model of Parkinson's disease. ***Neuron*** 2005; 46:857-868.

133. Neely MD, Sidell KR, Graham DG, Montine TJ. The lipid peroxidation product 4-hydroxynonenal inhibits neurite outgrowth, disrupts neuronal microtubules, and modifies cellular tubulin. ***J Neurochem*** 1999; 72:2323-2333.

134. Aldini G, Dalle-Donne I, Vistoli G, Maffei FR, Carini M. Covalent modification of actin by 4-hydroxy-trans-2-nonenal (HNE): LC-ESI-MS/MS evidence for Cys374 Michael adduction. ***J Mass Spectrom*** 2005; 40:946-954.

135. Ogburn KD, Bottiglieri T, Wang Z, Figueiredo-Pereira ME. Prostaglandin J2 reduces catechol-O-methyltransferase activity and enhances dopamine toxicity in neuronal cells. ***Neurobiol Dis*** 2006.

136. Wigley WC, Fabunmi RP, Lee MG, Marino CR, Muallem S, DeMartino GN ***et al***. Dynamic association of proteasomal machinery with the centrosome. ***J Cell Biol*** 1999; 145:481-490.

137. Ren Y, Zhao J, Feng J. Parkin binds to alpha/beta tubulin and increases their ubiquitination and degradation. ***J Neurosci*** 2003; 23:3316-3324.

138. Yang F, Jiang Q, Zhao J, Ren Y, Sutton MD, Feng J. Parkin stabilizes microtubules through strong binding mediated by three independent domains. ***J Biol Chem*** 2005; 280:17154-17162.

139. Alim MA, Ma QL, Takeda K, Aizawa T, Matsubara M, Nakamura M *et al*. Demonstration of a role for alpha-synuclein as a functional microtubule-associated protein. *J Alzheimers Dis* 2004; 6:435-442.

140. Cappelletti G, Pedrotti B, Maggioni MG, Maci R. Microtubule assembly is directly affected by MPP(+)in vitro. *Cell Biol Int* 2001; 25:981-984.

141. Diaz-Corrales FJ, Asanuma M, Miyazaki I, Miyoshi K, Ogawa N. Rotenone induces aggregation of gamma-tubulin protein and subsequent disorganization of the centrosome: Relevance to formation of inclusion bodies and neurodegeneration. *Neuroscience* 2005; 133:117-135.

142. Marshall LE, Himes RH. Rotenone inhibition of tubulin self-assembly. *Biochim Biophys Acta* 1978; 543:590-594.

143. Roy S, Zhang B, Lee VM, Trojanowski JQ. Axonal transport defects: a common theme in neurodegenerative diseases. *Acta Neuropathol (Berl)* 2005; 109:5-13.

144. Giri S, Rattan R, Singh AK, Singh I. The 15-deoxy-delta12,14-prostaglandin J2 inhibits the inflammatory response in primary rat astrocytes via down-regulating multiple steps in phosphatidylinositol 3-kinase-Akt-NF-kappaB-p300 pathway independent of peroxisome proliferator-activated receptor gamma. *J Immunol* 2004; 173:5196-5208.

145. Mrak RE, Landreth GE. PPARgamma, neuroinflammation, and disease. *J Neuroinflammation* 2004; 1:5.

146. Eucker J, Bangeroth K, Zavrski I, Krebbel H, Zang C, Heider U *et al*. Ligands of peroxisome proliferator-activated receptor gamma induce apoptosis in multiple myeloma. *Anticancer Drugs* 2004; 15:955-960.

147. Musiek ES, Milne GL, McLaughlin B, Morrow JD. Cyclopentenone eicosanoids as mediators of neurodegeneration: a pathogenic mechanism of oxidative stress-mediated and cyclooxygenase-mediated neurotoxicity. *Brain Pathol* 2005; 15:149-158.

148. Glickman MH, Rubin DM, Fried VA, Finley D. The regulatory particle of the Saccharomyces cerevisiae proteasome. *Mol Cell Biol* 1998; 18:3149-3162.

149. Figueiredo-Pereira ME, Berg KA, Wilk S. A new inhibitor of the chymotrypsin-like activity of the multicatalytic proteinase complex (20S proteasome) induces accumulation of ubiquitin- protein conjugates in a neuronal cell. ***J Neurochem*** 1994; 63:1578-1581.

150. Shibata T, Yamada T, Kondo M, Tanahashi N, Tanaka K, Nakamura H ***et al***. An endogenous electrophile that modulates the regulatory mechanism of protein turnover: inhibitory effects of 15-deoxy-delta(12,14)-prostaglandin J2 on proteasome. ***Biochemistry*** 2003; 42:13960-13968.

151. Ishii T, Sakurai T, Usami H, Uchida K. Oxidative modification of proteasome: identification of an oxidation-sensitive subunit in 26 s proteasome. ***Biochemistry*** 2005; 44:13893-13901.

152. Bajorek M, Finley D, Glickman MH. Proteasome disassembly and downregulation is correlated with viability during stationary phase. ***Curr Biol*** 2003; 13:1140-1144.

153. Martinez B, Perez-Castillo A, Santos A. The mitochondrial respiratory complex I is a target for 15-deoxy-delta 12,14-prostaglandin J2 action. ***J Lipid Res*** 2005; 46:7436-74473.

154. Allan SM, Rothwell NJ. Inflammation in central nervous system injury. ***Philos Trans R Soc Lond B Biol Sci*** 2003; 358:1669-1677.

155. Hirata Y, Hayashi H, Ito S, Kikawa Y, Ishibashi M, Sudo M ***et al***. Occurrence of 9-deoxy-delta 9,delta 12-13,14-dihydroprostaglandin D2 in human urine. ***J Biol Chem*** 1988; 263:16619-16625.